



Journal of Composites and Compounds

A review on the synthesis of the TiO₂-based photocatalyst for the environmental purification

Naghmeh Aboualigaledari ^{a*}, Mohammad Rahmani ^b

^a Department of Nanoscience, Joint School of Nanoscience and Nanoengineering (JSNN), University of North Carolina at Greensboro, Greensboro, North Carolina, United States

^b Department of Chemical Engineering, Amirkabir University of Technology, Tehran, Iran

ABSTRACT

TiO₂ as a photocatalyst has been widely investigated and applied in many fields such as fuel cells, sterilization, and environmental decontamination. Some efforts, such as operation pa-rameters, synthesis techniques, and improvements by doping have been made to improve its performance. To have a photocatalyst with high photocatalytic activity for environmental purification, the most important step is to know about the synthesis methods and the pa-rameters and conditions that lead to preparing a highly photocatalytic active photocatalyst. This article paves the way in selecting the best synthesizing technique. In this article, the most common synthesis techniques of TiO₂-based photocatalysts, including sol-gel, hydro-thermal, solvothermal, chemical vapor deposition, and physical vapor deposition have been reviewed. The most important results that have been achieved in the field of synthesis were collected.

©2021 JCC Research Group.

Peer review under responsibility of JCC Research Group

ARTICLE INFORMATION

Article history:

Received 18 November 2020

Received in revised form 25 January 2021

Accepted 29 February 2021

Keywords:

TiO₂-based photocatalyst

Liquid-phase processing

Physical production techniques

Environmental application

Table of contents

1. Introduction	25
2. Synthesis method	26
2.1. Sol-gel method	26
2.1.1. Modified sol-gel method	27
2.1.2. Preparation of photocatalysts with sol-gel method	27
2.2. Hydrothermal method	28
2.2.1. Photocatalysts preparation via hydrothermal method	30
2.3. CVD method	31
2.3.1. Preparation of photocatalysts by CVD method	35
2.4. PVD method	35
2.4.1. Pulsed laser deposition (PLD)	36
2.4.2 Electron-beam and ion-assisted electron-beam evaporation	36
2.4.3 Magnetron and reactive magnetron sputtering	36
2.4.4 Preparation of photocatalysts by PVD Method	36
3. Conclusions	37

1. Introduction

In the last decades, environmental purification has been one of the major challenges facing researchers [1-3]. Among the various methods used for environmental purification, semiconductor photocatalysis has been known as an effective and environmentally friendly method. TiO₂ has received increasing attention for photocatalysts application due to its nontoxicity, low cost, high oxidation power, and high chemical stability [4-25].

The recent nanotechnology development has shown that nanomaterials like nano-sized TiO₂ photocatalysts can exhibit high performance in environmental purification. A fast-developing field in environmental engineering is TiO₂ heterogeneous photocatalyst which has excellent potential for environmental purification. Fujishima and Honda discovered the photocatalyst performance of TiO₂ with the application of TiO₂-anode in the hydrolysis of water to hydrogen and oxygen [26, 27].

The metal of TiO₂ is present in nature in various forms. The oxides of TiO₂ have three various molecule structures including brookite, anatase, and rutile. Rutile is a pigment in white paints that has revealed

* Corresponding author: Naghmeh Aboualigaledari; E-mail: naghmeh.abuali@gmail.com

DOR: 20.1001.1.26765837.2021.3.6.4.7

<https://doi.org/10.52547/jcc.3.1.4>

This is an open access article under the CC BY license (<https://creativecommons.org/licenses/by/4.0>)

low photocatalytic performance, and anatase is more favorable in using as the photocatalytic cell. UV-light with 387 nm wavelength or lower is required for applying anatase [28].

Air conditioning (air purification), water purification, white tents, tunnel lightning, mirrors (anti-condensation), textile (anti-odor), ceramic tiles (self-cleaning, antibacterial), and self-cleaning glazing are some of the application of TiO_2 as photocatalyst. In addition to anti-septical action and air purifying in which the pollutants are reduced or oxidized, it is also used to prepare a self-cleaning material. This is because of the high surface hydrophilicity of TiO_2 which is the result of activation by UV-light [29].

Up to now, different methods have been reported to prepare TiO_2 and TiO_2 -based photocatalyst, including physical vapor deposition (PVD) [30], chemical vapor deposition (CVD) [31], solvothermal [32], hydrothermal [33–35], and sol-gel method [34]. Indeed, photocatalytic performance is especially influenced by some factors such as crystallinity, light adsorption ability, pore size, shape, and porosity. Since these factors are ultimately influenced by the preparation method, significant consideration should be done to study the effect of preparation methods, conditions, and parameters on photocatalytic performance [36]. Some reviews on the synthesis of TiO_2 -based materials exist [37–41], the works that have been done before 2011.

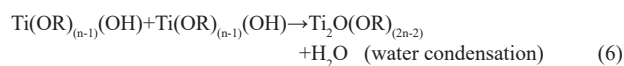
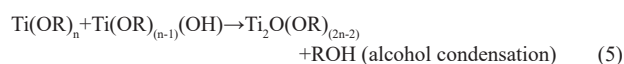
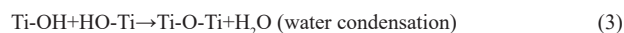
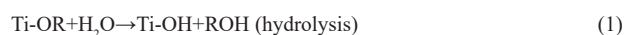
In this study, we review the latest advances in both liquid-phase processing and physical production techniques. Also, the precursors, surfactants, and solvents used in the synthesis process, as well as the operating parameters of synthesis were extensively studied. The results obtained from the publications, which can help to select the promotional materials and operating parameters in the synthesis process are shown.

2. Synthesis method

2.1 Sol-gel method

The sol-gel process is a wet chemical, a low-temperature method that is used for the synthesis of various nanostructures, especially metallic oxide nanoparticles. In this method, the precursors are dissolved in solvents and then converted into a gel via hydrolysis and polycondensation reactions, with or without the use of a catalyst, under heating and stirring conditions. Inorganic metal salt, metal-organic compounds, and miscellaneous titanium-containing [42] are the most common precursors used for TiO_2 nano photocatalyst synthesis. Principally, the sol-gel process includes the following steps: (a) preparation of the initial homogeneous solution, which is consisted of dissolution of the precursors in solvents (e.g., water, alcohol, and organic solvent). Sometimes it is necessary to use the combination of two solvents with a certain ratio, to get a homogeneous solution. For example, some metal alkoxides precursors (e.g. titanium tetraisopropoxide (TTIP)) are dissolved in an organic solvent (e.g. isopropyl alcohol) that is miscible with water and then dissolved in water [43]. (b) Hydrolysis of the initial homogeneous solution by adding water, under acidic, neutral, or basic conditions to provide a sol. Hydrolysis replaces an alkoxide ligand with a hydroxyl ligand or oxo ligands. Depending on the amount of water and catalyst present, hydrolysis reaction can be complete or partial. The sol complete hydrolysis forms a rigid gel, which can be heat-treated to form powders. The sol partial hydrolysis will provide a polymeric viscous liquid, which deposited on a substrate by dip coating or spin coating and thermally processed to obtain dense crystalline films [44]. Also, when the viscosity of the sol is adjusted into a specific range, ceramic fibers are produced. (c) Conversion of sol by changing the concentration or pH of the sol into a gel which can be an integrated discrete particles network or network polymer. Generally, gelation is involved condensation of hydroxyl and/or alkoxy groups that lead to the release of water or alcohol and then polymerization. A gel

that is produced from these processes is a nanostructure material. When the by-products (e.g., water or alcohol) are removed from this nanostructure via evaporation or the porosity of the gel is improved around the surfactant such as hexadecyltrimethyl, nanopore structure material is produced. The structure of the polymeric gel can be rigid with large void area (macropores) or weak with smaller void area (micropores). Different kinds of surfactants have been used for photocatalysts preparation, for instance, polyethylene glycol sorbitan monooleate surfactant has been used for the preparation of highly porous TiO_2 films. Another type of surfactant is lauryl amine hydrochloride (LAHC), which has been used to prepare mesoporous-assembled nano titania (TiO_2) thin films [45, 46]. As a different method, the gel can be formed from stabilized sol, in which the solvent of the precursor is usually water and very fast hydrolysis happen as a result of high water/alkoxide molar ratio, in this condition the synthesized nanoparticles agglomerate very rapidly, these aggregates can be broken up by peptizing agents such as HCl or NH_3 and as a result, the colloidal suspension is produced [47–51]. Complete (Eqs. (1)–(3)) and partial condensation and hydrolysis reactions (Eqs. (4)–(6)) of titanium alkoxide precursors are described by the following reactions:



Important factors that can affect the kinetics of the condensation and hydrolysis reactions of titanium alkoxide and titanium chlorides and will ultimately lead to the production of material with different structure, size, and morphology are water/titanium ratio, alcohol/titanium ratio, concentration, and nature of the precursors (alkoxy groups), pH, temperature, etc. According to the studies, the type of the alkoxy groups affects the size of the cluster formed [52]. The hydrolysis and diffusion rate of the alkoxides with higher alkyl groups is slow. Since polymerization is partial hydrolysis and diffusion-reaction, alkoxides with this property lead to the formation of oxide components with smaller sizes [53]. Hydrolysis and condensation rate are both influenced by pH. At acidic media, the hydrolysis reaction is improved, and hydrolysis is faster than condensation. Also, pH can influence the porosity, surface area, and pore size of the producing oxides. The water/titanium ratio has the greatest effect on the particle size and a higher water/titanium ratio leads to the faster gel formation of sol [48, 54]. (d) Aging: when the solvents are removed from the gel, keeping the pore structure stability is difficult. Normally in order to improve the strength of the links between particles, aging step, which takes a few hours or several days is necessary before draying step. (e) Drying: This step has involved the removal of solvent from the gel. There are two different methods for removing the solvent: 1- Drying the gel under ambient conditions. In this method shrinkage is obvious and the resulted material is called Xerogel which is a dense material with low porosity. 2- Drying the gel under hypercritical conditions. In this method, solid network collapse is minimized and the resulting material is called Aerogel which has high porosity. (f) Thermal treatment: To improve the structural stability and mechanical property, different kinds of thermal treatment such as sintering, densification, and calcinations are used. In a study done by Wetchakun et al, TiO_2 nanopar-

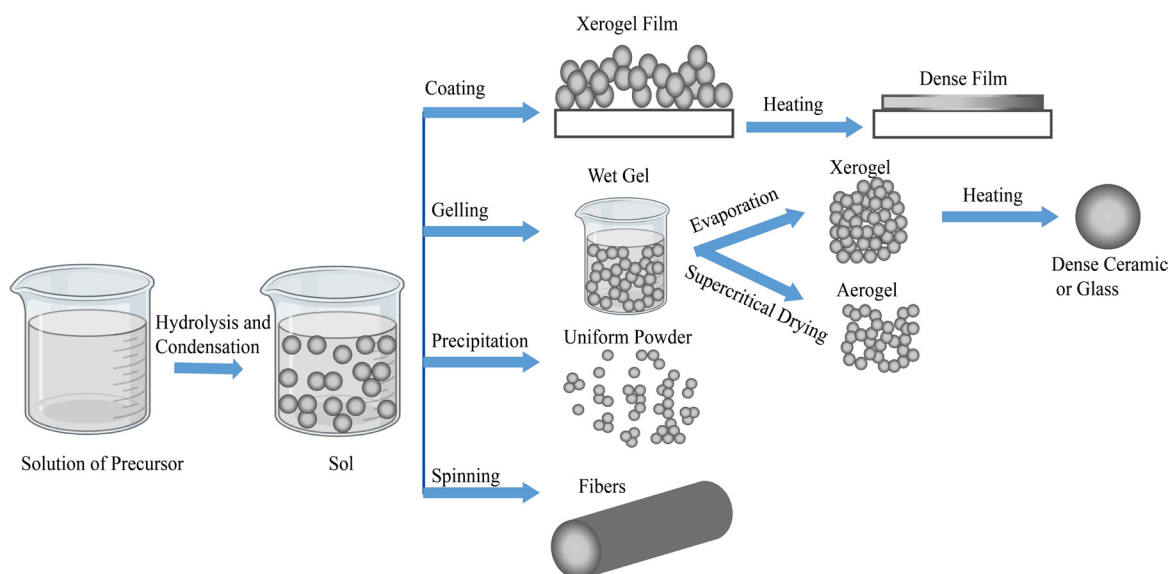


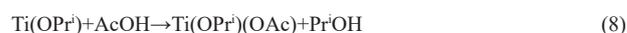
Fig. 1. Different sol-gel process steps to control the final morphology of the product.

ticles were prepared via the sol-gel method by titanium tetraisopropoxide as the titanium precursor, the results show that the calcination temperature can affect the average particle sizes of the nanoparticles and anatase to rutile transformation [55]. Different sol-gel process steps to control the final morphology of the product depicted in Fig. 1.

2.1.1 Modified sol-gel method

Generally, highly reactive titanium alkoxide precursors undergo aggressive and exothermic hydrolysis reaction and condensation reaction leads to the formation of the Ti-O-Ti network. This process can lead to the precipitation of undesired phases with particles of large size and uncontrolled structure. Also in the synthesis of nanosized TiO_2 powder, the high hydrolysis rate of titanium tetraisopropoxide can cause loss of optical and photocatalytic properties of nanosized TiO_2 material [56, 57]. To control the kinetics of hydrolysis and polycondensation reactions of titanium alkoxide precursors, some modifier ligands such as a diol, the carboxylic acid (e.g. acetic acid), and diketones (e.g. acetylacetone) compounds or other complex ligands are used [58, 59]. The most common modifiers used in the modification of the titanium alkoxide precursors are acetylacetone and acetic acid. Generally, the role of modifier ligands is to chemically react with alkoxide precursors and as a result, the reactivity of precursors is modified, and a new precursor is produced. Also, the shape and size of the primary particles which formed in the sol-gel of metal alkoxides are described by the interactions on the phase boundary, that is directed to the properties of ligand [60]. Acetyl acetone is a kind of hydroxylated strong complexing ligands (SCL) that has a reactive hydroxyl group. Due to this property, the reaction between acetylacetone and titanium alkoxide precursor results in the protonation of the oxygen atom in the alkoxide ligand, and as a result alcohol and a modified alkoxide precursor are produced. The reactions of titanium tetraisopropoxide with acetylacetone (enolic form) are described in Eq. (7) [58, 60, 61]. Another modifier is acetic acid. As it is shown in Eq. (8)-(9) the reactions of titanium tetraisopropoxide with acetic acid lead to the production of new precursors. In this reaction, due to the replacement of the alkoxy groups bonded to titanium by acetate groups, Ti-OAc and ROH are formed. Modification of titanium tetraisopropoxide $\text{Ti}(\text{O-Pr})_4$ with glacial acetic acid decrease the availability of groups which condense and hydrolyze easily by stable complex formation, which its structure was specified to be $\text{Ti}(\text{OCOCH}_3)(\text{OPr})_2$ [58, 62]. Esterification reaction (Eq. (10)) of AcOH with alcohol leads to the releasing of water in the solution. In the esterification reaction, titanium alkoxide precursor can be hydrolyzed with water molecules through esterification reaction

followed by condensation reaction to form Ti-O-Ti [63, 64]. The esterification reaction has several drawbacks for example: if the reaction is not controlled the generated water can lead to precursor condensation reaction. The hydrolysis and direct condensation reaction which is another route of the formation of Ti-O-Ti condensed bridge is described in Eqs. (11)-(12) [56-58, 65].



2.1.2 Preparation of photocatalysts with sol-gel method

Several investigations have been done due to the photocatalyst preparation via the sol-gel method, some of these synthesis processes are described as following:

Titanium sol was prepared by TiCl_4 acid hydrolysis, in this route pH of the medium was adjusted by NH_4OH , at pH=6 to 7, followed by peptization of precipitates with HNO_3 . Stable titania sol was prepared at the molar ratio $[\text{H}^+]/[\text{Ti}]=0.5, 1, 1.5, \text{ and } 2$ with strong stirring at 70°C for 24 h. To prepared $\text{SiO}_2\text{-TiO}_2$ (the content of SiO_2 was 10 wt%) nanoparticles photocatalyst, the appropriate amount of tetraethylorthosilicate (TEOS) solution was dropped in the sol of titania followed by drying and calcination at $400\text{-}700^\circ\text{C}$ for 1-3 h [66]. TiO_2 based catalyst exhibited the highest photocatalytic performance because of lowest crystallite size, highest surface area, and better crystallization, at calcination temperature of 400°C for 3 h. The optimum condition of $[\text{H}^+]/[\text{Ti}]$ ratio is taken at 0.5. When the pH value increased from 6 to 7, this led to an increase in surface area.

Both Ni, Co, and Fe-doped TiO_2 and pure TiO_2 samples were prepared by the alkoxide route of the method of sol-gel. The precursor of TiO_2 was tetraethyl orthotitanate and the solvent was the absolute ethanol. The titanium alkoxide hydrolysis took place at room temperature with a final pH=6 of the solution. Undoped TiO_2 and 0.5, 1, and 2 wt% Co, Fe, or/and Ni-doped nanopowders of TiO_2 were synthesized. The

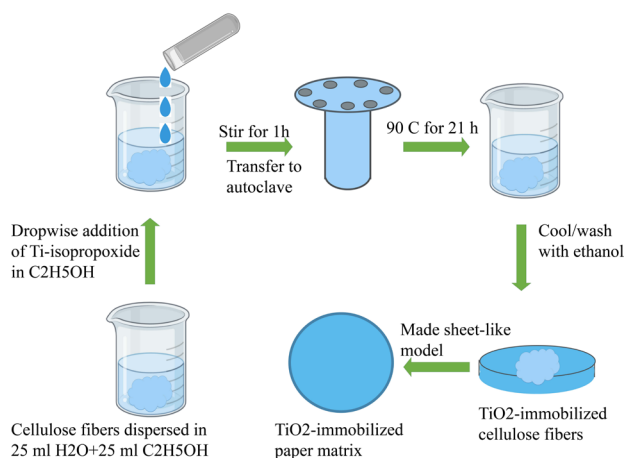


Fig. 2. Schematic diagram of a hydrothermal method.

compositions with 0.5 wt% dopants were chosen for this work. The prepared sols dried at 80 °C and the xerogels were thermally treated with a heating rate of 1 °C/min at 400 °C (1 h plateau). The sample with 0.5 wt% Fe dopant concentration thermally treated at 400 °C showed the best photocatalytic performance for nitrobenzene removal from water [67].

To prepare N-doped TiO₂ samples decorated with N-doped graphene, 17 mL of tetrabutyl titanate was mixed with 30 mL of ethanol with stirring for 30 min (solution A). A mixture of 28.32 mL absolute ethyl alcohol, 7.2 mL distilled water, 20 mL of acetic acid, a specified proportion of carbamide and graphene oxide with various graphene proportion of 0.5wt%, 1wt%, 3wt%, and 5wt% before adding another 20 mL of acetic acid was added to solution A with 30 min of stirring. The aging and drying condition was 24 h and 100 °C, respectively. The samples were calcination at (400, 500, and 600 °C) in the furnace under the N₂ atmosphere for 2.5 h. The results suggested that N-RGO (0.5wt%)/N-TiO₂-400 °C showed the best photocatalytic efficiency for the decomposition of methylene blue (MB) [68]. In another work, the preparation of mesoporous Fe₂O₃/TiO₂ in the presence of Pluronic P123 as the structure-directing agent was done by addition of iron (III) nitrate nonahydrate (1.52 g) and titanium tetraisopropoxide (5.18 mL) into a mixture of Pluronic P123 (1 g) and ethanol (60 mL). In this method pH of the medium was adjusted by a solution of ammonia (8 mL) and distilled water (36 mL), to pH around 10. After 24 h stirring, the obtained mixture for nucleation the precipitated was hold in the dark overnight. To get a fine powder, the product was centrifuged and dried at 100 °C and then calcination at 400 °C for 5 h in an N₂ atmosphere. Meso-30 wt% Fe₂O₃/TiO₂ showed highest photocatalytic activity for 4-chlorophenol degradation [69]. A summary of TiO₂ and TiO₂-based photocatalysts prepared via sol-gel or modified sol-gel method are reported in Table 1.

2.2 Hydrothermal method

The hydrothermal synthesis can be defined as any heterogeneous reaction in an aqueous media performed at a pressure higher than 1 atm and above room temperature [70]. It should be noticed that with a non-aqueous solvent (e.g., n-butyl alcohol, ethanol, methanol, toluene, etc), the process is referred to as the solvothermal method. In comparison to the other methods, the solvothermal method involves much milder conditions and softer chemistry conducted at lower temperatures [71]. Hydrothermal and solvothermal are techniques to produce TiO₂

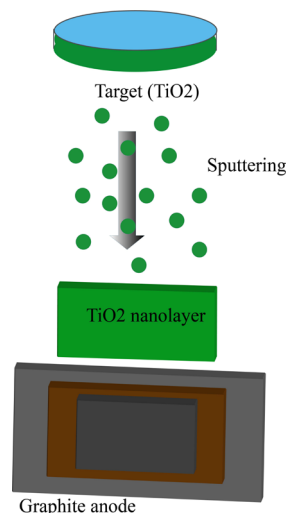


Fig. 3. Chemical vapor deposition mechanism.

and TiO₂-based nano photocatalysts with different morphology such as nanosheets [72], nanofibers [73], nanotubes [74], films [75], nanoparticles [76, 77], nanorods [78, 79], powder [80, 81], and to process nanocomposites materials [82–86]. The common Ti-source used in the synthesis process of nano photocatalysts via hydrothermal and solvothermal methods are titanyl sulfate (TiOSO₄) [83], titanium (IV) butoxide (TBOT, Ti(OC₄H₉)₄) [72, 82, 87], TiCl₄ [76, 79, 81, 88], titanium tetraisopropoxide (TTIP, Ti(OCH(CH₃)₂)₄) [73, 89], Ti(SO₄)₂ [80, 90], titanium (IV) n-butoxide (TNB, Ti(OBu)₄) [91], TiO₂-P25 [92] and TiCl₃ [93]. Precursors which are used in the hydrothermal method are administered in the form of solutions, gels, and suspensions. These precursors are heated at a temperature range between (100–200 °C) and pressure (P < 100 bars), in autoclaves usually with Teflon liners. After the reaction occurred in the autoclave, the autoclave is cooled and some process such as centrifuging, drying, washing, etc is done.

In the hydrothermal method, some organic or inorganic mineralizers are used to control pH, also mineralizers with high concentrations (e.g., 10 m), used to promote solubility. For example, mineralizers such as NaOH, KOH, HCl, HNO₃, HCOOH, and H₂SO₄ are used in the synthesis of TiO₂ nanoparticles. Also, to control the shape of the nanomaterial, some other additives or shape control agents are used [94–97]. For instance, to prepare TiO₂ with a specific nanostructure, some surfactant molecules such as ammonia, diamine, dodecane diamine (DDA) [98], and triethanolamine [99] are used. As another example, in a system based on ethylene glycol and titanium tetra isopropoxide, the hydrothermal method of the base system could fabricate nanowires. In this system, the addition of ethylenediamine (EDA) with different concentrations led to a change in the shape of nanomaterial from nanowire to nanorods, nanofibers, and arrays [71]. To enhance the reaction kinetics or make a new material, the hydrothermal techniques can be hybridized with other processes such as microwaves, ultrasound, electrochemistry, etc [95].

A technique to prepare thin films or porous TiO₂ powder is the sol-gel method which has a drawback that involves deposition or calcined sol-gel-synthesized TiO₂ can readily form particles aggregates rather than a periodic and continuous inorganic framework. The hydrothermal method with low reaction temperature has been specified to solve this problem. The other advantage of the hydrothermal method for nanocrystalline state synthesis is the possibility to produce the material with uniform composition, phase, and microstructure [75, 76, 100]. Although the Hydrothermal synthesis process seems to be very simple, some pa-

Table 1.Summary of TiO₂ and TiO₂-based photocatalysts prepared via sol-gel or modified sol-gel method

Catalyst-shape	Method	The material used for the preparation	Model compound	Operating condition	Main results	Ref
Nanoparticles of TiO ₂ -CS, Pd/TiO ₂ , as well as Pd/TiO ₂ -CS	Modified sol-gel	TiO₂ Precursor: TiC ₁₆ H ₃₆ O ₄ (titanium sec-butoxide) The material used in the synthesis process: Solvent for TiO ₂ precursor: ethanol, HCl, and double-distilled water Precipitation agent: ammonia solution Pd source and solvent: PdCl ₂ (Pd to TiO ₂ molar ratio: 0.03), distilled water (50 mL) CS source and solvent: 1 g of CS (CS to TiO ₂ molar ratio: 0.03), aqueous acetic acid solution (100 mL of 5%) pH controller (pH 9): ammonia solution	MB	Pd/TiO ₂ : Drying: at 100 °C overnight Calcination: for 5 h at 550 °C TiO ₂ -CS: Drying: at 100 °C for 24 h Calcination: at 550 °C for 5 h in air Light source: Xenon lamp	• Chitosan can prevent the agglomeration of TiO ₂ nanoparticles • Photocatalytic activity: Pd/ TiO ₂ < TiO ₂ -CS < Pd/ TiO ₂ -CS.	[168]
TiO ₂ -P25-nanocomposite films	Peroxotitanic acid (PTA) modified sol-gel	TiO₂ Precursor: TTIP (5 mL) The material used in the synthesis process: Solvents for TiO ₂ Precursor: isopropanol (20 mL) Hydrolysis agent: deionized water (100 mL) PTA sol: dissolving the precipitate in 20 mL of aqueous H ₂ O ₂ Surface modifier: 0.3 g 10% PEG solution TiO ₂ -P25 film preparation: substrate based on borosilicate glass with the dimension of 4.5 × 39.5 × 0.2 cm and sol of P25 (4 wt.%)	Reactive Red 222 (RR222)	Drying: 100 °C in the oven for 1h Calcination: 500 °C for 2 h Light source: UV-C lamp	The photocatalytic efficiency of TiO ₂ -P25 increase due to effective charge transfer	[169]
CNS-TiO ₂ -nanoparticles	Sol-gel	TiO₂ Precursor: TTIP The material used in the synthesis process: Solvents for TiO ₂ precursor: isopropyl alcohol solution Hydrolysis agent: deionized water Precursor and solvents for CNS-TiO ₂ preparation: thiourea, double distilled water.	Amidoblack-10B dye (AB-10B)	Drying: 80 °C, in oven Calcination: 400 °C Light source: solar light	Co-doped TiO ₂ activity under visible light irradiation is higher compared to pure TiO ₂	[43]
N-doped TiO ₂	Sol-gel reverse micelle (SGRM)	TiO₂ precursor: titanium (IV) 2-ethyl-1,3-hexanedioate (15.71 g) The material used in the synthesis process: Solvents for TiO ₂ precursor: isopropyl alcohol (30 mL) Material for micelle reverse solution preparation: cyclohexane (16 mL), aqueous solution of Na ₂ EDTA (14 mL) and TritonX100 (50 µliter)	MB	Heating: 70 °C for 60 min Aging: 24 h Drying: 80 °C for 8 h Calcination: for 1 h at 500 °C in static air with a 5 °C/min heating rate Light source: Mercury/Xenon lamp (λ=400 nm)	Optimum condition: N/Ti atomic ratio=0.05	[42]
TiO ₂ - fibers	Sol-gel	TiO₂ Precursor: TBOT The material used in the Synthesis process: Solvent for TiO ₂ precursor: anhydrous alcohol (TBT to EtOH molar ratio: 1:3) Surfactant: solution of PVP and HCl (26 mL) in absolute alcohol	Formaldehyde	Stirring: 2h Oil bath temperature: 110-140 °C Calcination: 500 °C for 90 min Light source: UV (λ=254 nm)	Optimum condition: H ₂ O:TBOT molar ratio ≤ 2	[170]
H-PVA/TiO ₂ -composite films	Sol-gel	TiO₂ Precursor: TBOT The material used in the synthesis process: Solvent for TiO ₂ precursor: EtOH, AcOH Hydrolysis agent: deionized water (100 mL) and HCl (0.3 mL) Preparation of glass slides based on H-PVA/TiO ₂ : (75 mm × 25 mm × 1 mm), the mass ratio of PVA/ TiO ₂ : 1/5	Rhodamine B (RhB)	TiO ₂ preparation: Stirring: 2h, 70 °C Aging: 48 h at room temperature Preparation of H-PVA/ TiO ₂ : Heat-treating: at 12-240°C for 4h in an N ₂ gas flow Light source: Tungsten-Halogen lamp	Optimum condition: 180 °C and 16.7 mass% of polymer content	[167]
TiO ₂ -powder	Sol-gel	TiO₂ Precursor: TiCl ₄ The material used in the synthesis process: Solvent for TiO ₂ precursor: Ethanol/water (volume ratio of 4:1) Hydrolysis agent: Ammonia (pH=7.5)	Phenol	Calcination: 450 °C for 4 h Drying: 80 °C Light source: sunny day of summer (April–May)	19.6 nm species size demonstrate good photocatalytic activity under solar irradiation	[171]

Table 1. (Continued)

Catalyst-shape	Method	The material used for the preparation	Model compound	Operating condition	Main results	Ref
TiO ₂ -Fe ₂ O ₃	Sol-gel	TiO₂ Precursor: TiOCl ₂ The material used in the synthesis process: FeCl ₃ ·6H ₂ O and FeCl ₂ ·4H ₂ O (Fe ³⁺ : Fe ²⁺ =1:2) were added in distilled water and then added to 20 mL TiOCl ₂ . Ammonia solution was used to control pH at 9	MB	Aging: at 80 °C for 4 h and then settled at room temperature for 12 h with gentle stirring Drying: 80 °C for 24 h in the thermal oven Calcination: for 2 h at 400, 600 and 800 °C in a box furnace Light source: 100 W Halogen lamp emitting wavelengths=350-1050 nm	Optimum condition: 5 wt% Fe ₂ O ₃ and calcination at 600 °C	[172]
Zirconium doped TiO ₂ -nanopowder	Controlled sol-gel route based on halide free non-aqueous solvent	Precursor: TTIP (20 mL) The material used in the synthesis process: Solvents for TiO ₂ precursor: 2-methoxy ethanol (40 mL) Zirconium precursor: Zirconium-oxy-nitrate-hydrate (0.831 g, 1.754 g, and 2.785 g) Quenchers: potassium iodide (KI), sodium azide (NA), parabenzoquinone (BQ), and dimethyl sulphoxide (DMSO) pH controller (pH 3): HNO ₃ and KOH	MB, RhB	Drying: using IR lamp (250 watt) and then pulverization Calcination: 450 °C for 1 h Light source: high-pressure ultra vitalux lamp (300 W, peak wavelength: 365 nm)	Doping of 10 at.% Zr leading to obtaining TiO ₂ nano-powder with the size of 11 nm rendering energy gap of 3.33 eV increase photocatalytic efficiency	[173]
TiO ₂ -ZnO	Sol-gel	TiO₂ Precursor: TBOT The material used in the synthesis process: ZnO precursor: zinc nitrate (Zn (NO ₃) ₂ ·6H ₂ O) Catalyst: citric acid Solvent: deionized water	H ₂ generation	Heating: 100 °C on a hot plate Annealing: for 5 h at 500 °C in a static atmosphere using a 1 °C/min heating rate Light source: UV	Optimum condition: 10% ZnO-TiO ₂	[174]
TiO ₂ /activated carbon	Sol-gel	TiO₂ Precursor: TTIP (2.87 mL) The material used in the synthesis process: Solvents for TiO ₂ precursor: anhydrous isopropanol (10 mL) Activated carbon: 250 mg, Solvent for activated carbon: water (5 mL)	Tetracycline	Stirring: 5 min at room temperature Drying: 100 °C for 12 h Pyrolysis: under N ₂ gas flow for 2 h at 500 °C Drying: 100 °C for 24 h Light source: UV (18 W)	•Better electronic and structural features were observed in TiO ₂ /AC • Bandgap energy: 3.04 eV anatase phase crystal size: 8.53 nm, and SBET: 129 m ² /g	[175]
N-doped TiO ₂	Sol-gel	TiO₂ Precursor: TBOT (10 mL) The material used in the synthesis process: Solvent for TiO ₂ precursor: anhydrous ethanol (20 mL) Stabilizer: acetylacetone (2.5 mL) N source: ethylenediamine (N:Ti molar ratios: 0, 3.65, 5.21, 7.29, 18.23, 36.47, 72.94, 109.41)	MO and H ₂ evolution	Stirring: 4 h Aging: 3 days Drying: 60 °C for 5 days Calcination: 300-600 °C for 1-3 h	Optimum condition: ethylenediamine to sintering temperature of 500 °C and sol volume ratio of 1:1	[34]

rameters such as the type and source of precursors, the hydrothermal condition (e.g. reaction temperature and time), and the washing procedure, play important roles in controlling the structure of the produced photocatalysts. [74]. The schematic diagram of a hydrothermal method of synthesis TiO₂ matrix is depicted in Fig.2.

2.2.1 Photocatalysts preparation via hydrothermal method

F-doped anatase TiO₂ nanoparticles were prepared by adding dropwise 2.2 mL TiCl₄ to a solution of 2 mL HF (40%) and 36 mL solution of HCl (1.0 M) under vigorous stirring for 30 min. Then the resulted solution was placed in a 50 mL stainless-steel autoclave and maintained at 120-180 °C for 4-12 h. After the autoclave was cooled to room temperature, the resulted sample was collected by centrifugation, washed with distilled water various times, and dried in an oven at 80 °C. The presence of HF led to the formation of the F-doped shuttle-like anatase nanostructures of TiO₂ [76].

In another study, nanoparticles of TiO₂ were synthesized by titanium tetraisopropoxide hydrolysis using tetramethylamine (TMA) as a pep-

tizer in the hydrothermal technique. In this route, white precipitates of hydroxous oxides were prepared by adding titanium isopropoxide solution (water/TTIP molar (R) ratio=100) into a solution of trimethylamine and water with vigorous stirring at 25°C. The mixture was stirred for 2 h. Then the resulted solution (200 mL) was placed in a 250 mL Teflon container maintained in a vessel and heated for 4 h at 120-200 °C. The resulted in TiO₂ particles were separated using a centrifuge at 10,000 rpm for 10 min, after that washed in distilled water, and dried for 12 h at 105 °C, at last calcined for 3 h at 200-800 °C. The result showed that titania particles synthesized at 170 °C and calcined at 600 °C, have the highest performance in the orange II photocatalytic decomposition under UV light [77].

In yet another study, nanofibers were synthesized from low-cost (0.5-0.7 dollar/kg) natural ilmenite mineral (FeTiO₃) by a simple hydrothermal method. In this route, ilmenite mineral (5 g) and 10 M aqueous solution of NaOH (200 mL) were placed in an autoclave, heated, and stirred for 72 h at 120 °C. Then the mixture was cooled to room temperature, and washed with 0.1 M aqueous solution of HCl and deionized water (DI) several times, and dried at 100 °C for 12 h. The nanofibers calcined

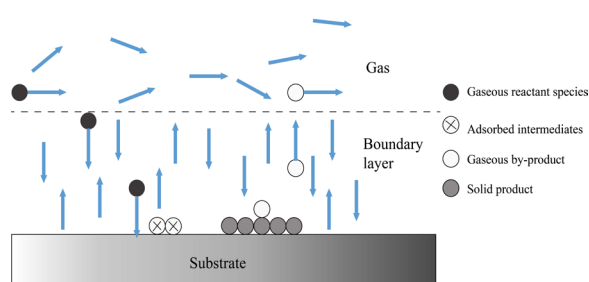


Fig. 4. Schematic of physical vapor deposition for TiO₂ coating.

at 300–400 °C presented TiO₂, the nanofibers calcined at 500 °C presented a mixture of anatase and TiO₂ and the nanofibers calcined at 600–1000 °C presented the mixture of Fe₂O₃, tri-crystalline of anatase, and rutile [73]. A summary of TiO₂ and TiO₂-based photocatalysts synthesized via hydrothermal and solvothermal method are reported in Table 2.

2.3 CVD method

Chemical vapor deposition (CVD) is one of the photocatalyst preparation methods. In this process, one or more volatile precursors are evaporated to the carrier gasses and transfer into the reaction chamber. Depending on the reactions, which can occur in the gas phase (homogeneous reaction) or near/on a heated substrate (heterogeneous reaction), either powder or solid thin films are formed. Thermal decomposition or reaction of gas or vapor phase species occurs at a temperature range between (500–1000 °C) [101–103]. Preparation of powder and film includes several steps. It can be noticed that the main steps for nanoparticle formation are: (a) nucleus formation, (b) nucleus growth, and (c) collection of nanosized powder [104]. Also, the main steps for thin film deposition on the substrate can be described as follow: (a) volatile precursors are evaporated into carrier gas and then transferred by the gas into the reactor; (b) gaseous reactions happen in the reaction zone; (c) the mass transfer of the reactants is occurred to the heated substrate; (d) adsorption of the reactants occurs on the substrate; (e) surface diffusion of sediments is occurred and cussed by surface chemical reactions, nucleation, and layers growth and (f) deposition of unreacted precursors and by-products from the reaction zone.

There are different parameters, which can control the deposition rate and quality of a film resulting from a CVD process, such as 1- Carrier gas (reactant gas or inert gas including H₂, N₂, and Ar). These kinds of gases have different prominent features and any of these features have a typical effect. For instance, the gas flow rate has an effect on the deposition rate, source temperature (effect on the deposition rate and dispersion of supporting materials), total pressure gas flows, and carrier gas composition. 2- Type of the precursors and type and temperature of the substrates, which have effects on the temperature of crystal structure transition through TiO₂ preparation process. 3- Experimental conditions such as deposition time (long deposition time can cause several problems, for example, energy consumption) and synthesis temperature (influence on the visible light performance of TiO₂ photocatalyst, species of supporting material, and percentage of anatase and rutile content). 4- Reactor design [105–110].

The selection of a suitable precursor is an essential requirement of the metalorganic chemical vapor deposition (MOCVD) process. To select a suitable precursor, several parameters should be considered. For instance, adequate volatility, thermal stability, conventionally, low hazardous risk, high chemical purity, clean decomposition, and long shelf life. The common Ti-precursors used to synthesis the TiO₂ and TiO₂-based photocatalysts by the CVD method are halides such as TiCl₄ [111–

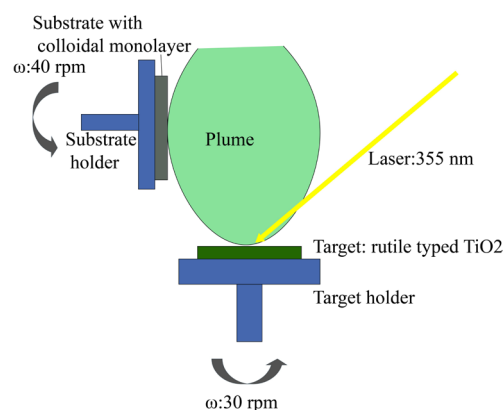


Fig. 5. Schematic illustration of PLD process.

114], alkoxides such as TTIP [105, 115–124], TBOT [101], and titanium nitrate. The metalorganic precursors such as titanium isopropoxide (Ti(OPr)₃), are less toxic and pyrophoric and offer the advantage of lower deposition and reaction temperatures than halides. Titanium isopropoxide includes an unsaturated four-coordinate Ti(IV) center, that is very reactive to moisture and air, and can cause problems in handling and storage, particularly in solution-based liquid injection MOCVD applications. TiCl₄ is toxic and needs safety installations and particular equipment. Its use can result in severe chloride contamination in CVD films. Several ligands such as β-ketoesters, β-keto amides, malonates, and aminoalkoxides have been used to synthesize the mixed alkoxide complexes of titanium. These ligands increase the sublimation rate and decrease the decomposition temperature. Also to reduce the sensitivity of moisture of the Ti-alkoxide precursors, chelating β-diketone groups and bidentate donor functionalized ligands including 2-dimethylaminoethanol or diolates including 2-methyl pentane-2, 4-diolate, have been inserted to improve the Ti(IV) coordination sphere saturation [125–127]. As an example of the photocatalysts, which are produced from complex precursors in a chemical vapor deposition and photo-assisted CVD process, titania thin films were synthesized by titanium isopropoxide (Ti(OPr)₃) and titanium [bis (dipivaloylmethanate) diisopropoxide] (Ti(DPM)₂(OPri)₂) complex compound precursors. The result showed that two crystalline forms, anatase and rutile, could be synthesized by these precursors, and also it has been observed that surface composition is different from that of the bulk in the film [128].

As mentioned above, chemical reactions can happen in both the gas phase (homogeneous reactions), which leads to powder formation (poor film morphology) and on the surface of the substrate (heterogeneous process). As the decomposition reaction is strongly dependent on the pressure, it is true to say that the selection of the low pressure (~Torr) can lead to heterogeneous reactions. Various types of CVD reactions consist of thermal decomposition reactions (pyrolysis reactions), reduction reaction, oxidation, hydrolysis, oxidation, nitride and carbide formation, and disproportionation [90]. Pyrolysis is involved the thermal dissociation of a gaseous compound into solid material and a gaseous reaction product. This reaction does not attack the substrate chemically. Pyrolysis reaction of a halide is described in Eq. (13). According to reduction reaction (Eq. (14)), in the presence of an adequate amount of reducing agent such as hydrogen, chemistry occurs primarily on the substrate. Oxidation (Eq. (15)) and hydrolysis reactions (Eq. (16)) is greatly used to deposit oxide materials. The most common oxidizing agent which is used in these reactions is oxygen and water. In disproportionation reaction (Eq. (17)), the oxidation number of an element both increases and decreases through the formation of two new species.



Table 2.

Summary of TiO₂ and TiO₂-based photocatalysts synthesized via hydrothermal and solvothermal method

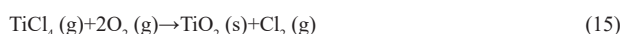
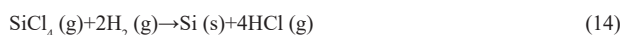
Photocatalyst-shape	Method	The material used for the preparation	Model compound	Operating condition	Main results	Ref.
WO ₃ /TiO ₂	Hydrothermal	TiO₂ Precursor: titanyl sulfate (TiOSO ₄) The material used in the synthesis process: double distilled water, titanyl sulfate (weight ratio= 4:5:1), and absolute ethanol WO ₃ precursor: ammonium tungstate	MO and 2, 4-dichlorophenol (2, 4-DCP)	Stirring: 24 h at 25 °C Autoclave conditions: 140 °C, 16 h, Teflon-inner-liner stainless steel Washing: water and ethanol Drying: 40–50 °C (overnight) Calcination: 500 °C Light source: visible and UV light (λ < 420 nm)	Optimum condition: 5.0% composite	[83]
SnS ₂ /TiO ₂	Solvothermal	TiO₂ Precursor: TBT Material used in the synthesis process: SnCl ₄ ·5H ₂ O (5 mmol), thioacetamide (10 mmol) and 5 vol% acetic acid aqueous solution (40 mL). SnS ₂ nanoparticles (0.4 g), TBT (0.5–2.0 mL) and a solution (38.0–39.5 mL) of ethanol (34.0 mL) and acetic acid (4.0 mL)	Aqueous Cr (VI)	The hydrothermal reaction for SnS ₂ : 150 °C for 24 h Autoclave conditions: 180 °C, 12 h Cooling: at room temperature Washing: deionized water Drying: 100 °C, 4 h, in vacuum Light source: visible light (λ > 420 nm)	Optimum condition: SnS ₂ /TiO ₂ -B with the TiO ₂ content of 25.5 mass%	[82]
TiO ₂ -nanosheets	Hydrothermal	TiO₂ Precursor: TBOT The material used in the synthesis process: distilled water (80 mL), NH ₃ OH, and a solution of titanium (IV) butoxide mixing with acetylacetone	concentration	Stirring: 5 minutes Autoclave conditions: 120 °C for 12 h, Thai made Cooling: at room temperature Washing: distilled water and 0.1 M of HCl Drying: 100 °C for 12 h in an oven Heating: 300, 400, 500, 600, 700 and 800 °C for 2 h	Specific surface area: 360.28 m ² /g, average pore diameter: 3–5 nm, pore volume 0.275 cm ³ /g	[72]
N, S-doped TiO ₂ -powders	Hydrothermal	TiO₂ Precursor: Ti(SO ₄) ₂ Materials used in the synthesis process: CS (NH ₂) ₂ , and an of Ti(SO ₄) ₂ (12.0 g), and distilled water (100 mL) solution	MO	Oil-bath temperature: 120 °C Hydrothermal treatment: 24 h Washing: distilled water Drying: 60 °C for 10 h, in a vacuum Calcination: 400, 500, 600, and 700 °C in the air for 3 h Light source: sunshine irradiation	Optimum condition: 3% N, S-TiO ₂ calcined at 500 °C	[80]
Core-shell TiO ₂ @ ZnIn ₂ S ₄	Hydrothermal-ultrasonication	TiO₂ Precursor: TiO ₂ Materials used in the synthesis process: TiO ₂ , deionized water (60 mL), ZnCl ₂ (1 mmol), In(NO ₃) ₃ ·4.5H ₂ O (2 mmol), and excessive thioacetamide (TAA, 6 mmol)	MB	Autoclave conditions: 160 °C for 6 h Cooling: at room temperature Washing: distilled water and absolute ethanol Drying: 80 °C for 6 h in a vacuum Light source: visible light (λ = 420 nm)	Compared to TiO ₂ , Core-shell TiO ₂ @ ZnIn ₂ S ₄ showed higher photocatalytic activity	[176]
La/TiO ₂ -graphene composites	Hydrothermal	TiO₂ Precursor: TBT Materials used in the synthesis process: a suspension of TBT (15 mL), ethanol (80 mL), distilled water (40 mL at pH 3.0), and La(NO ₃) ₃ ·6H ₂ O. A solution of graphene oxide (20 mg), distilled water (80 mL), ethanol (40 mL), and TiO ₂ (200 mg)	MB	Synthesis of TiO ₂ nanopowder: Stirring: 1 h Autoclave condition: 180 °C for 6 h Washing: deionized water Drying: 100 °C in the vacuum oven for 12 h Calcination: 450 °C Synthesis of La/TiO ₂ graphene composites: Stirring: 2 h Autoclave conditions: 120 °C for 3 h Washing: deionized water Drying: 70 °C for 12 h Light source: Visible light (λ ≥ 420 nm)	Photocatalytic activity of La/TiO ₂ -graphene composites was higher than TiO ₂	[177]

Table 2. (Continued)

Photocatalyst-shape	Method	The material used for the preparation	Model compound	Operating condition	Main results	Ref.
(N–F) codoped TiO ₂ -nanobelts	Solvothermal	TiO₂ Precursor: TBT Materials used in the synthesis process: Step1: TBT (2.2 mL), a mixture of sodium chloride solution (0.4 mL 0.1 M) and ethanol (100 mL). Step2: TiO ₂ (0.8 g), ammonium fluoride (0.37 g), 10 M sodium hydroxide solution (50 mL)	MO	Step1: Aging: for 24 h in a static condition Drying: 80 °C in air Step 2: Stirring: about 30 min Autoclave conditions:180 °C for 72 h Cooling: down to room temperature Washing: with ethanol and deionized water Drying: in the air at 80 °C Light source: visible solar irradiation ($\lambda \geq 420$ nm).	Mesopores like a prison, wormhole-like, enhanced absorption of light and larger surface area in the case of N-F codoping increasing the photocatalytic performance	[178]
Ag/TiO ₂ /ZnO composite particles	Hydrothermal	TiO₂ Precursor: P25(TiO ₂) Materials used in the synthesis process: aqueous suspension of the mixture of TiO ₂ (20 mg) in ethanol (10 mL), 0.058 M bis-hexamethylene triamine (40 mL), 5.8810- 3 M AgNO ₃ (10 mL), and 0.063 M zinc nitrate hexahydrate (40 mL)	The aqueous solution of reactive black 5	Stirring: for 1 h Autoclave condition:140 °C for 2 h Cooling: at room temperature Washing: alcohol and distilled water Drying: 130 °C for 12 h	Ag/TiO ₂ /ZnO composite decrease the rate of electron-hole separation and prevent the loss of photocatalyst during recovery	[179]
Anatase nano-TiO ₂ -powder	Hydrothermal	TiO₂ Precursor: TiCl ₄ Materials used in the synthesis process: TiCl ₄ (20 mL), ethanol (200 mL), H ₂ O ₂ (80 mL), and 10 wt% ammonia	RhB	Autoclave condition:140 °C for 2 h Drying: 60 °C in vacuum Washing: distilled water Light source: (λ_{\max} =553 nm)	Increasing the hydrothermal synthesis time and the sol concentration lead to an increase in particle size	[81]
Nitrogen-doped titania -nanoparticles	Micro-wave-assisted solvothermal process	TiO ₂ Precursor:TiCl ₃ Materials used in the synthesis process: hexamethylenetetramine (HMT, 2 g) and 20 wt% TiCl ₃ solutions (10.75 cm ³), 12.5 cm ³ of distilled water, methanol, and ethanol	MO	Autoclave condition: 160-230 °C for 5min using a 1000 W microwave reaction apparatus Washing: distilled water and acetone Vacuum drying: at 80 °C overnight Light source: simulated solar radiation Xenon-lamp (λ_{\max} =465 nm)	The reaction time could be reduced resulting from the high microwave irradiation heating	[93]
Urchin-like titania	One-step hydrothermal method	TiO₂ precursor: TiO ₂ particles Materials used in the synthesis process: 10 M NaOH solution with TiO ₂ : NaOH molar ratio of 1:333	MO	Stirring: 10 min at room temperature Autoclave condition: 100 mL Teflon autoclave and an H ₂ O ₂ solution (30 wt%) was added followed by rinsing with hydrochloric (0.1 M) Drying: 10 h at 50 °C Annealing: at 550 °C for 2 h in air and reducing atmospheres (10% H ₂ + 90% Ar) respectively	<ul style="list-style-type: none"> At temperatures of 130 and 150 °C, thick and small holes were present on the urchin-like surface. Adding H₂O₂ form finer urchin-like surface and hydrogenation increase photocatalytic efficiency 	[180]
TiO ₂ /graphene quantum dots	One-step hydrothermal	TiO₂ precursor: TiO ₂ particles Materials used in the synthesis process: 0.5 g of TiO ₂ nanoparticles, a suspension of 15 mg of 1,3,6-trinitropyrene (TNP), and 0.2 M NaOH aqueous solution (80 mL)	Hydrogen evolution	Ultrasonication: (150W, 50 kHz) for 4 h and additional sonication for 2 h Autoclave condition: Teflon-lined autoclave (100 mL), 200 °C for 10 h Washing: water and ethanol Drying: in the air for overnight Light source: 250 W high-pressure mercury lamp	TiO ₂ /graphene quantum dots H ₂ evolution rate and photocurrent response at optimal GQDs content is 7 and 3 times higher than TiO ₂	[181]
G-C ₃ N ₄ /TiO ₂ hetero-junction composites	Hydrothermal	TiO₂ precursor: TiCl ₄ Materials used in the synthesis process: 0.5 mL of TiCl ₄ , a solution of melamine containing 0.5, 1, 2, 3, or 4 g melamine, and 60 mL of DI	RhB	Stirring: 30 min and then at 3-5 °C for 2 h in an ice bath Autoclave condition: stainless steel autoclave lined with Teflon (100 mL). 180 °C for 4 h Drying: 100 °C for 10 h and then heating in the crucible for 2 h at 550 °C at a 5 °C/min rate in a muffle furnace under air atmosphere	<ul style="list-style-type: none"> For 0.5 mL of TiCl₄, optimum melamine content was 3 g Specific surface area: up to 115.6 m²/g 	[182]

Table 2. (Continued)

Photocatalyst-shape	Method	The material used for the preparation	Model compound	Operating condition	Main results	Ref.
Bi-TiO ₂ nanotube/graphene composites	One-step hydrothermal	TiO₂ precursor: Degussa P25 Materials used in the synthesis process: 1 g of Degussa P25, a suspension of GO (2 wt%), and 30 mL of double distilled. various amount of bismuth nitrate and NaOH	Dinoseb (phenolic herbicide) and MB	Autoclave condition: Teflon-lined autoclave and heated for 24 h at 140 °C Washing: double distilled water followed by acid washing with HCl (0.1 M) Drying: 80 °C for 16 h, dry overnight at 80 °C Annealing process: 350 °C for 6 h Light source: visible light 500 W (9500 lumens) linear halogen lamp	2-wt% bismuth shows improvement in photocatalytic activity	[6, 183]
Graphene/TiO ₂ /CdS nanocomposites	Hydrothermal	TiO₂ precursor: TBT Materials used in the synthesis process: GO (15 mg), TBT (2.63 mmol), diethylene glycol (60 mL). A solution of acetone (180 mL) and deionized water (600 μL). A suspension of Cd(NO ₃) ₂ ·4H ₂ O/L-cysteine (0.2/0.6, 0.4/1.2, 0.6/1.8 mmol) and deionized water (80 mL)	MB and parachlorophenol (4-CP)	Stirring: 12 h at room temperature another stirring 1.5 h Washing: water/ethanol Autoclave condition: 120 °C for 12 h Light source: a visible-light	The surface area of GO-TiO ₂ -0.55CdS (157.5 m ² /g) result in higher photocatalytic activity	[184]



The CVD process can be operated in either a close or open system. Closed systems can be utilized for reversible reactions, for example, metal purification. However, it can be said that close systems are less common in comparison with open systems. In open systems, the carrier gasses flow through the reactor and after deposition, by-products and unreacted precursors are carried by carrier gas, and then go out from the reactor [129]. Main equipment in the open systems can be classified into three basic components: 1- Delivery system, which is used to produce vapor precursors and deliver them to the reactor. 2- The effluent gas handling system. To provide the low pressure or high vacuum pressure for the CVD method, some systems such as a mechanical pump (van pump) are used [105]. Many precursors used in the CVD method are toxic and pyrophoric, in this respect, a liquid nitrogen trap is employed to neutralize or entrap the hazardous by-product and unreacted precursors, before being released to the environment [107, 130]. 3- CVD reactor.

Conventional CVD reactors including distributing and delivering reactive gases through a substrate, and a system of heating with temperature control. Regarding the performance of CVD reactors, it is highly important to be considered, that precursors must be injected into the reactor, also carrier gasses with a certain flow rate and temperature must be injected into the reactor. The volatile precursors are carried out by carrier gas toward the substrate and then decomposed on the surface of the substrate, after that the extra vapor precursors and exhausted gasses are removed from the reactor, then the reactor is purged by inert gas [105–108, 131]. There are several types of CVD methods, which are classified based on the activation energy of the reaction. Various activation energies can be included: thermal (RF heating, infrared radiation, and resistive heating), photons (UV lamp-laser), and plasma (DC current-frequency, pulses-microwave). Thermally activated CVD is called TCVD, photonic activated CVD is called LCVD and plasmatic activated

CVD is called PECVD (plasma-enhanced CVD). Another type of CVD method is metalorganic CVD (MOCVD) which uses metalorganics as the precursor. The pressure for MOCVD is usually around 10³–10⁵ Pa and the temperature range is between ~300–800 °C. In this type of reactor, reactants are volatile at relatively low temperatures.

Thermally activated CVD is a usual CVD process in which thermal energy in a cold wall or hot-wall reactor by inorganic chemical precursors led to the initiation of the chemical reactions. A hot wall reactor is usually tubular and surrounded by an isothermal furnace and is used mostly for an exothermic reaction. The advantage of this reactor is close temperature control and the disadvantage is that deposition can occur on the wall of the reactor because the wall and the substrate have the same temperature. The cold wall reactor is bell-jar shaped and used for endothermic reactions. In this reactor, the substrate is heated directly either by electricity (induction) or by glowing heating, as a result, the rest of the reactor remains cold and the substrate has the highest temperature. The processes of thermally activated CVD can be subdivided based on the pressure range of deposition. The operating pressure can be considered as (a) low-pressure CVD (LPCVD), the pressure range is between 10–1000 Pa; (b) atmosphere pressure (APCVD) and (c) high vacuum pressure (HPCVD), the pressure is less than 10^{−5} Pa. The difference between LPCVD/UHVCVD and APCVD is the ratio of the mass transport velocity and the velocity of reaction on the surface. It can be said that the diffusion of a gas is inversely proportional to the pressure [125, 132].

In PECVD temperature is between 100–700 °C and pressure is 1–80 Pa. PECVD processes by metal-organic precursors have gained attention due to their potential in lowering the deposition temperatures, as a result, this process is used in the coating of the temperature-sensitive substrates. In a DC plasma-assisted and thermally activated CVD process by titanium isopropoxide as a precursor, the TiO₂ film deposition has been under investigation. The result shows that the pulsed DC plasma has several advantages such as: nanostructured of crystalline TiO₂ are deposited at a lower temperature, the plasma-assisted CVD produced dense microstructure even in amorphous deposits and enhanced desorption of residual surface contamination [123].

The LCVD is a CVD derivative in which the global heat source for the furnace is replaced with a localized spot heated by a laser [133].

The use of precursors with better deposition routes is more important than the utilization of less volatile precursors, in this respect, some

Table 3.
Summary of TiO₂ and TiO₂-based photocatalysts prepared via CVD method

Photocatalyst-shape	Reactor design	Model compound	Operating conditions	Main results	Ref.
TiO ₂ films covered by noble metal nanoparticles silver, platinum	Radiofrequency (RF) low-pressure PECVD reactor	Acid Orange 7 (AO7)	Precursor: TTIP Substrate: glass slide and silicon wafer Temperatures: 40, 300 °C Liquid heated evaporator temperature: 50 °C Oxygen flow rate: 25 to 200 sccm Working gas: a TTIP vapors and oxygen mixture Pressure: 8–20 Pa Bias on the substrate: about -50V at 20 W Light source: UV-A lamp (15 W, λ=365 nm)	Treated or untreated films synthesized at higher temperature (300 °C) showed enhanced antibacterial properties	[122]
TiO ₂ thin film deposited on silica gel powder	Radiofrequency circulating fluidized bed PECVD reactor	MB	Precursor: TTIP Deposition temperature: 250 °C Supplying power: 13.56 MHz Bubbler temperature: 95 °C Light source: ultraviolet lamp (15 W/cm ² , λ=365 nm)	The optimum condition for anatase phase deposition was 3.6 vol.% of O ₂ , 0.4 g/min of TTIP, and 8.18 vol.% of Ar	[121]
TiO ₂ coating of activated carbon	AP-MOCVD (hot-wall reactor)	MO	Precursor: TBOT Deposition temperature: 600 °C Light source: UV lamp (1.2 15 mW/cm ² , λ=356 nm)	<ul style="list-style-type: none"> The particles size is ranging from 10 to 50 nm The optimum loading of TiO₂ was 12 wt% 	[101]
N-doped titanium thin film	APCVD (custom-built, horizontal cold wall reactor)	Stearic acid	Precursor: TiCl ₄ Deposition temperature: 500 °C Bubbler temperature: 40 °C and 70 °C	Selective doping at the interstitial site (ionization 400 eV by XPS) shows a dominant impact on the enhancement of photocatalysis	[112]
Needle-like TiO ₂ / WO _{3-x}	APCVD-cold wall reactor	Stearic acid	Precursor: TiCl ₄ Deposition temperature: 500 °C Bubbler temperature: 200 °C Light source: UVC light (200 W Xenon lamp, λ=254 nm)	The increase in activity of films is explained in terms of effective vectorial charge separation at the interface of the two oxide semiconductors	[113]

delivery systems are used to generate vapor precursors and deliver them to the reactor. Different types of delivery systems are classified based on the phase of the precursors (liquid, solid, and gas). The method for gas precursor delivery is to use a cylinder containing the right composition of the precursor with a mass flow controller to control the vapor phase concentration. The liquid precursors with low pressures must be heated in an oil bath or placed in a bubbling chamber, to evaporate to their evaporation temperature. Also, carrier gasses must be used to deliver volatile precursors to the reactor [132, 134]. It can be said that the precursor's flow rate should be controlled by adapting the temperature of the bubbling chamber or/and the flow rate of carrier gasses [103]. If the vapor pressure of the liquid reactant is specified, its partial pressure may be designed and controlled by controlling the flow rate and volume of the carrier gas. On the other hand, like a flash vaporization method, the flow rate of the precursors must be controlled by a syringe pump or other equipment, and carrier gas with mass flow controlled can be used to deliver volatile precursors towards the reactor [105, 132]. If the phase of the precursors is solid precursors, the precursor must be sublimated and then transferred by the carrier gas to the reactor [107].

2.3.1 Preparation of photocatalysts by CVD Method

TiO₂ nanoparticles were coated onto a glass bead using a CVD method with T-junction apparatus and using TTIP as a precursor. The precursor was vaporized in a bubbler using argon gas at 90 °C and then carried with carrier gasses (argon and nitrogen) through an alumina tube which was heated at 900 °C and connected to a horizontal T-junction containing soda lime glass beads. The deposition time was regulated to 10, 30, 60, and 120 min. The result showed that the sample with the 60 min coating time had the best photocatalytic performance (~52%) for the decomposition of acetaldehyde. Another result is that TiO₂ nanoparticles were deposited with a uniform shape onto the glass bead, and the coating

time was decreased with this simple process [116].

TiO₂ /silica gel photocatalyst was synthesis by the CVD method, according to three steps: (a) the support materials pretreatment by adding water dropwise to silica gel and then drying for 20 min at 110 °C; (b) CVD reaction and (c) calcination at 500 °C for 3 h in airflow. In the synthesis process, TTIP was stored in a separate container (bubbler at 80 °C) and introduced into the reactor of CVD (300 °C) by the carrier gas (nitrogen) under vacuum. The result showed that the size for all the TiO₂ /silica gel samples is uniform in the 10–20 nm range [120]. The mechanism of chemical vapor deposition is illustrated in Fig.3. A summary of TiO₂ and TiO₂-based photocatalysts prepared via the CVD method is reported in Table 3.

2.4 PVD method

In processes of physical vapor deposition (PVD), the coating is deposited in a vacuum using condensation from a flux of ionized or neutral metal atoms. The basic PVD processes fall into two general categories: (a) thermal methods (evaporation and electron-beam evaporation) and (b) mechanical methods (cathodic sputtering). For the evaporation process, the substance to be evaporated is heated in an evacuated chamber so that it attains a gaseous state. The coating material is moved along the transport area and condenses on the substrate surface. For sputtering, atoms are ejected mechanically from a target with the ions impact or energetic neutral atoms.

Electron-beam evaporation (EBE) [135–137], ion-assisted electron-beam evaporation [138–140], pulsed laser deposition (PLD) [31, 141], radio frequency (RF) magnetron sputtering [142–145], direct current (DC) magnetron sputtering [146–148], and pulse magnetron sputtering [149, 150] are the common PVD methods, which are used to synthesis photocatalysts. Fundamental of PVD process is like CVD, except that in PVD method the raw materials, which are going to be deposited

start in solid form. Also in comparison with the CVD method, the PVD process does not produce harmful by-products and it can be noticed that the operating temperature of the PVD method (200 to 300 °C) is less than the CVD method [151, 152]. The main disadvantage of processes of PVD (with EB-PVD exception) is the low deposition rates. The schematic of physical vapor deposition for TiO₂ coating is depicted in Fig.4.

2.4.1 Pulsed laser deposition (PLD)

In the PLD method, a focused pulsed-laser beam illuminates one or more targets and thin films are prepared by the ablation of these targets. There are different parameters affecting film properties such as laser fluence, pressure, background gas, substrate temperature, target-to-substrate distance, wavelength, and pulse duration [153]. The experimental apparatus used in the PLD method contains: a deposition chamber that is evacuated to a base pressure using a mechanical pump and a Cryopump and the chamber is filled with gasses (e.g., oxygen, nitrogen, etc). Other components are a pulsed laser (Nd: YAG laser, KrF laser), which is used to irradiate the target, and a substrate (part to be coated) that is set apart from the target and heated by an instrument (e.g., IR lamp or laser). The advantages of the PLD technique are that this method causes the growth of high-quality thin-film materials. PLD as a thin film deposition technique possesses some disadvantages including droplet deposition on the film and the formation of non-homogeneous films [154]. Several investigations have been done on photocatalyst synthesis via the PLD method. For example, nitrogen-doped titanium oxide photocatalyst was synthesized using PLD. With this regard, the TiN target in a gas mixture of N₂/O₂ was used. According to the results, the N₂ ratio in the gas mixture and target material have significant effects on the film structure and properties. Additionally, the absorption edges of the films shifted from 320 nm to 360 nm for TiO₂ and TiO_{2-x}N_x films, respectively [155]. Mn-doped ZnO/TiO₂ multilayer nanostructures (photocatalyst) were deposited on Si (100) substrates by this method. To prepare the nanostructure, a multi-target carousel system was used following by post-growing annealing in O₂ or N₂ atmosphere at a pressure of 1 bar and temperatures of 400–800 °C. It was found that the thicknesses of grown nanostructures by the pulsed laser deposition technique were about 2 and 15 nm [156]. Fig.5 shows a schematic illustration of the PLD process.

2.4.2 Electron-beam and ion-assisted electron-beam evaporation

In EBE, to evaporate the material, a beam of electrons with high kinetic energy is directed to the target material. On the surface of the components or substrates, the evaporated material is condensed causing the formation of a deposit. In the EBE method, the deposition rate can be varied simply by adjusting the beam current and during the deposition process also it does not particularly need the specific gas atmosphere. The other advantages of the EBE method are the high deposition rate, excellent economy, and practicability [157–159]. EBE is one of the methods that are preferred among different physical vapor deposition techniques to deposit TiO₂ films to achieve high-quality optical thin films [140]. An annealing treatment is essentially required after deposition to control the morphology, structure, and thereafter photocatalytic activity of the films that have been prepared [158]. EBE unit consists of main components namely, EB-gun assembly, a substrate that is usually held with a rotating substrate holder, a (vacuum) chamber, and a target [160]. EBE method is used in the deposition of thin films on a substrate. For example, on a substrate of quartz glass with a temperature of 200 °C, TiO₂ thin-film was deposited at oxygen gas pressure accounting for 6.7 × 10⁻³ Pa. TiO₂ was used as a target, and the base pressure of the chamber was 8.0 × 10⁻⁴ Pa. The results exhibited higher photocatalytic activity of GO/TiO₂ in the UV-violet compared to the visible range [136]. Using an ion-assisted EBE system, TiO_xC_y films were deposited by using carbon monoxide (CO) and the source material of rutile TiO₂ powder

flowing through a dopant source (ion gun). According to the results, the CO ion beam can produce TiO_xC_y films with visible-light responsiveness [139]. Another result is that the film crystallinity deteriorated because of the increasing ion-beam current.

2.4.3 Magnetron and reactive magnetron sputtering

In the sputtering method, materials are eliminated from objects by transferring energy in energetic atomic projectile collisions. In magnetron sputtering, the magnetron field can be created by permanent magnets, electromagnets, or a combination of both [161]. Magnetron sputtering of TiO₂ films is one of the most favorable techniques because this industrial process provides the ability of large-area deposition rendering good adhesion to substrates. Also, with this technique, high-quality TiO₂ films could be obtained even at low substrate temperatures. Both DC and RF sputtering techniques have attracted extensive attention recently because of the very smooth surface that is achieved by sputtering [143, 161–163]. In the magnetron sputtering technique, the sputtering gas is an inert gas (e.g., Ar) and in the reactive magnetron sputtering a second gas (O₂), which can react with the target material is added to the sputtering gas. In DC reactive sputtering method, plasma is created between the anode (substrate holder) and the cathode, and positive ions in plasma sputter off the atoms from a target (cathode) that is connected to a potential source. These atoms react further with the particles of the reactive gas and deposit on the substrate under an oxidized form [164]. Properties and structure of the DC-magnetron-sputtered TiO₂ films can be controlled and modified by regulating process parameters including coating thickness, sputtering gas Ar: O₂ ratio, sputtering power, and sputtering pressure [165].

2.4.4 Preparation of photocatalysts by PVD Method

Pansila et al. [166] used the DC reactive magnetron sputtering method with a variation in the sputtering power to synthesize TiO₂ films. The Ti target (120 mm) was sputtered in the Ar + O₂ gas mixture. In this study, the deposition of the TiO₂ thin films was carried out on the unheated substrate (silicon wafer) at 210 W and 230 W sputtering power. The deposition happened in the vacuum chamber (at 3 h, base pressure: 5.0 × 10⁻⁵ mbar and total pressure: 5.0 × 10⁻³ mbar). The result showed that the sputtering power strongly affected the TiO₂ thin film crystalline structure. With an increase in the sputtering power of the cathode, the TiO₂ thin film structure was transformed from anatase to mixed structure of anatase/rutile.

In a work done by Huang et al. [143], the influence of the deposition parameters, such as substrate temperature, argon-oxygen ratio (O₂/(Ar + O₂)), RF power, and deposition time, on the decomposition of methylene blue, was studied. In this study, titanium oxide films were applied on non-alkali glass (temperature: 100 °C) by RF magnetron sputtering with the base pressure of 0.67 × 10⁻³ Pa and sputtering power of 20 W using a Ti metal target. Sputtering and reactive gases were Ar and O₂. It was found that parameters that had a dominant influence on the absorbance of MB were argon-oxygen ratio and RF power.

In another study done by Nair et al. [142], the deposition of TiO₂ thin films was performed onto cleaned quartz substrates by RF magnetron sputtering method following post-annealing at 873 K using TiO₂ ceramic target, which was synthesized by pelletized TiO₂ powder sintering for 4 h at 1673 K. The authors investigated the influence of sputtering pressure and the RF power on the optical and structural properties of the films. The results indicated that the films contain anatase phase, also the results show that a decrease in sputtering pressure and the increase in RF power leads to a decrease in the optical bandgap.

Su-Shia et al. [167] employed the simultaneous DC magnetron sputtering of W and RF magnetron sputtering of TiO₂ to heavy doping of the TiO₂ films with W (TiO₂:W). This type of deposition method offers

Table 4.
Summary of TiO₂ and TiO_x-based photocatalyst prepared by PVD method

Photocatalyst	Method	Model compound	Synthesis condition	Main results	Ref.
TiO ₂ thin films deposited on quartz glass	Electron-beam evaporation	MB	Target: TiO ₂ (99.99% pure) Substrate-to-target distance: 650 mm Evaporator pressure: 6 × 10 ⁻⁶ Torr Working oxygen gas pressure: 5 × 10 ⁻⁵ Torr Deposition temperature: 200 °C The voltage of electron gun: 7.0 kV Current: 200 mA Substrate rotate vertical axis: 15 rpm Deposition rate: 1.50-2.05 Å/s, at an incident angle of 0-75° Annealing: 600 °C in air, 1 h Light source: black-light lamps (20 W) with λ=352 nm	Incident deposition angle up to 60° led to the enhanced photocatalytic activity while a further increase to 75° decreased the photocatalytic activity resulted from a lack of the crystalline phase	[135]
TiO ₂ /SiO _x /TiO _x multi-layers deposited on quartz glass	Electron-beam evaporation	MB	Deposited temperature: 200 °C Distance between the substrate and target: 580 mm Base pressure: 6.0 × 10 ⁻⁶ Torr The partial pressure of oxygen: 2.5 × 10 ⁻⁵ Torr for the TiO _x layer, 6.0 × 10 ⁻⁵ Torr for the SiO ₂ layer, and 5.0 × 10 ⁻⁵ Torr for the TiO ₂ layer deposition The voltage of electron gun: 7.0 kV Current: 110 mA for SiO ₂ , and 220 mA for TiO ₂ Substrate rotate vertical axis: 15 rpm Deposition rate: 0.25 nm/s, 1.00 nm/s and 0.25 nm/s Annealing: in air and at 600 °C for 1 h Light source: 20W-black-light lamps, λ=352 nm	Due to more trap levels in the SiO _x (80 nm) inter-layer and higher surface roughness, the TiO ₂ /SiO _x (80 nm)/TiO ₂ multi-layer showed promising photocatalytic activity	[137]
Thin films based on Bi: TiO ₂	Pulsed laser deposition and thermal evaporation	Malachite green solution	Laser: Nd: YAG with emission at the third harmonic (355 nm), pulse duration: 10 ns, focal length spherical lens: 60 cm, incidence angle: 45°, laser fluence: 10.0 J/cm ² Base pressure: 2 × 10 ⁻⁵ Torr Substrate-to-target distance: 5 cm Light source: Hg lamp, λ=404 nm	Bi: TiO ₂ thin films reduced the bandgap energy and also favored the formation of segregated anatase and b-Bi ₂ O ₃ phases	[31]
TiO ₂ films deposited on non-alkali glass	RF magnetron sputtering	MB	Target: TiO ₂ with 50.8 mm diameter and 99.995% purity Deposition time: 180 min Base pressure: 5.0 × 10 ⁻⁶ Torr Gas: O ₂ (99.995%), Ar (99.995%) Distance between the substrate and target: 8 cm Rotate vertical axis of substrate: 10 rpm Light source: blacklight lamp, λ=365 nm	The optimal condition was 10 mTorr sputtering pressure, power of 200 W, 50% argon-oxygen ratio, and 450 °C for substrate temperature	[185]
Boron-doped titanium dioxide (B-TiO ₂) films	Reactive magnetron co-sputtering	MB	Target and power: 99.99% titanium (SDIC) metal, 200 W, 99.5% TiB ₂ , 30, 60, 90, 120, 150 and 180 W Substrates: glass or fused quartz slides and polished Si (100) wafers Distance between the substrate and the targets: 100 mm Base pressure: 4.0 × 10 ⁻⁵ Pa or lower Substrate temperature: 100 °C Gas flow rates and pressure: 8 sccm for O ₂ and 20 sccm for Ar, 4.0 × 10 ⁻¹ Pa (3.0 × 10 ⁻³ Torr). Thicknesses of the films: 300 nm Light Source: UV	Ti ₂ BO ₂ enhanced the photocatalytic activity of TiO ₂ under visible-light	[186, 187]

the capability of changing the W content in a wide range. A summary of TiO₂ and TiO_x-based photocatalyst prepared by the PVD method are reported in Table 4.

3. Conclusions

TiO₂ is a promising material for environmental applications. Several parameters such as suitable pore size, high specific surface area, good crystallinity, and porosity, also shape can be very effective to achieve more efficient photocatalytic activity of TiO₂. Also, modification of TiO₂ with various materials is a good method to achieve better photoactivity and enhance the visible light absorption ability. The photocatalytic activity and light absorption ability are influenced by preparation meth-

ods, parameters, and conditions. In the future researchers can focus on physical production techniques. As these techniques still need effort and investigation.

Acknowledgments

This research did not receive any specific grant from funding agencies in the public, commercial, or not-for-profit sectors.

Conflict of interest

The authors declare that there is no conflict of interest.

REFERENCES

[1] A. Jafari Rad, Synthesis of copper oxide nanoparticles on activated carbon for

- pollutant removal in Tartrazine structure, *Journal of Composites and Compounds* 2(3) (2020) 99–104.
- [2] A. Abuchenari, K. Hardani, S. Abazari, F. Naghdi, M. Ahmady Keleshteri, A. Jamavari, A. Modarresi Chaharhehi, Clay-reinforced nanocomposites for the slow release of chemical fertilizers and water retention, *Journal of Composites and Compounds* 2(3) (2020) 85–91.
- [3] S. Askari, M. Ghashang, G. Sohrabi, Synthesis and mechanical properties of $\text{Bi}_2\text{O}_3\text{-Al}_2\text{Bi}_2\text{O}_3$ nanopowders, *Journal of Composites and Compounds* 2(5) (2020) 171–174.
- [4] B. Cheng, Y. Le, J. Yu, Preparation and enhanced photocatalytic activity of Ag@TiO_2 core-shell nanocomposite nanowires, *Journal of Hazardous Materials* 177(1–3) (2010) 971–977.
- [5] H. Jing, Q. Cheng, J.M. Weller, X.S. Chu, Q.H. Wang, C.K. Chan, Synthesis of TiO_2 nanosheet photocatalysts from exfoliation of TiS_2 and hydrothermal treatment, *Journal of Materials Research* 33(21) (2018) 3540–3548.
- [6] H. Mao, Z. Fei, C. Bian, L. Yu, S. Chen, Y. Qian, Facile synthesis of high-performance photocatalysts based on Ag/TiO_2 composites, *Ceramics International* 45(9) (2019) 12586–12589.
- [7] S. Liu, Y. Zhang, Synthesis of CPVC-modified $\text{SnS}_2/\text{TiO}_2$ composite with improved visible light-driven photocatalysis, *Materials Research Bulletin* 135 (2021) 111125.
- [8] S. Narzary, K. Alamelu, V. Raja, B.M. Jaffar Ali, Visible light active, magnetically retrievable $\text{Fe}_3\text{O}_4@\text{SiO}_2@\text{g-C}_3\text{N}_4/\text{TiO}_2$ nanocomposite as efficient photocatalyst for removal of dye pollutants, *Journal of Environmental Chemical Engineering* 8(5) (2020) 104373.
- [9] Y. Shen, P. Zhou, S. Zhao, A. Li, Y. Chen, J. Bai, C. Han, D. Wei, Y. Ao, Synthesis of high-efficient TiO_2 /clinoptilolite photocatalyst for complete degradation of xanthate, *Minerals Engineering* 159 (2020) 106640.
- [10] S. Alberti, V. Caratto, D. Peddis, C. Belviso, M. Ferretti, Synthesis and characterization of a new photocatalyst based on TiO_2 nanoparticles supported on a magnetic zeolite obtained from iron and steel industrial waste, *Journal of Alloys and Compounds* 797 (2019) 820–825.
- [11] S. Ali, Z. Li, S. Chen, A. Zada, I. Khan, I. Khan, W. Ali, S. Shaheen, Y. Qu, L. Jing, Synthesis of activated carbon-supported TiO_2 -based nano-photocatalysts with well recycling for efficiently degrading high-concentration pollutants, *Catalysis Today* 335 (2019) 557–564.
- [12] J.C. Lopes, M.J. Sampaio, B. Rosa, M.J. Lima, J.L. Faria, C.G. Silva, Role of TiO_2 -based photocatalysts on the synthesis of the pharmaceutical precursor benzhydrol by UVA-LED radiation, *Journal of Photochemistry and Photobiology A: Chemistry* 391 (2020) 112350.
- [13] S. Saroj, L. Singh, S.V. Singh, Solution-combustion synthesis of anion (iodine) doped TiO_2 nanoparticles for photocatalytic degradation of Direct Blue 199 dye and regeneration of used photocatalyst, *Journal of Photochemistry and Photobiology A: Chemistry* 396 (2020) 112532.
- [14] H. Zhang, X. Wang, N. Li, J. Xia, Q. Meng, J. Ding, J. Lu, Synthesis and characterization of TiO_2 /graphene oxide nanocomposites for photoreduction of heavy metal ions in reverse osmosis concentrate, *Royal Society of Chemistry Advances* 8(60) (2018) 34241–34251.
- [15] X. Yu, H. Qiu, B. Wang, Q. Meng, S. Sun, Y. Tang, K. Zhao, A ternary photocatalyst of all-solid-state Z-scheme $\text{TiO}_2\text{-Au-BiOBr}$ for efficiently degrading various dyes, *Journal of Alloys and Compounds* 839 (2020) 155597.
- [16] N. Yaacob, G.P. Sean, N.A.M. Nazri, A.F. Ismail, M.N. Zainol Abidin, M.N. Subramaniam, Simultaneous oily wastewater adsorption and photodegradation by $\text{ZrO}_2\text{-TiO}_2$ heterojunction photocatalysts, *Journal of Water Process Engineering* 39 (2021) 101644.
- [17] B. Zhang, X. He, X. Ma, Q. Chen, G. Liu, Y. Zhou, D. Ma, C. Cui, J. Ma, Y. Xin, In situ synthesis of ultrafine TiO_2 nanoparticles modified g- C_3N_4 heterojunction photocatalyst with enhanced photocatalytic activity, *Separation and Purification Technology* 247 (2020) 116932.
- [18] N. Sedaghati, A. Habibi-Yangjeh, S. Asadzadeh-Khaneghah, S. Ghosh, Integration of oxygen vacancy rich- TiO_2 with BiOI and $\text{Ag}_2\text{Si}_2\text{O}_7$: Ternary p-n-n photocatalysts with greatly increased performances for degradation of organic contaminants, *Colloids and Surfaces A: Physicochemical and Engineering Aspects* 613 (2021) 126101.
- [19] J. Abdi, M. Yahyanezhad, S. Sakhaie, M. Vossoughi, I. Alemzadeh, Synthesis of porous TiO_2 / ZrO_2 photocatalyst derived from zirconium metal organic framework for degradation of organic pollutants under visible light irradiation, *Journal of Environmental Chemical Engineering* 7(3) (2019) 103096.
- [20] X. Wei, C. Wang, S. Ding, K. Yang, F. Tian, F. Li, One-step synthesis of Ag nanoparticles/carbon dots/ TiO_2 nanotube arrays composite photocatalyst with enhanced photocatalytic activity, *Journal of Environmental Chemical Engineering* 9(1) (2021) 104729.
- [21] D. Boczar, T. Łęcki, M. Skompska, Visible-light driven $\text{Fe}_3\text{O}_4/\text{TiO}_2$ /Au photocatalyst – synthesis, characterization and application for methyl orange photodegradation, *Journal of Electroanalytical Chemistry* 859 (2020) 113829.
- [22] Y.P. Bhoi, F. Fang, X. Zhou, Y. Li, X. Sun, J. Wang, W. Huang, Single step combustion synthesis of novel $\text{Fe}_2\text{TiO}_5/\alpha\text{-Fe}_2\text{O}_3/\text{TiO}_2$ ternary photocatalyst with combined double type-II cascade charge migration processes and efficient photocatalytic activity, *Applied Surface Science* 525 (2020) 146571.
- [23] A. Shahnazi, M.R. Nabid, R. Sedghi, B. Heidari, A thermosensitive molecularly imprinted poly-NIPAM coated MWCNTs/ TiO_2 photocatalyst for the preferential removal of pendimethalin pesticide from wastewater, *Journal of Photochemistry and Photobiology A: Chemistry* 402 (2020) 112802.
- [24] M. Sabri, A. Habibi-Yangjeh, H. Chand, V. Krishnan, Activation of persulfate by novel TiO_2 / FeOCl photocatalyst under visible light: Facile synthesis and high photocatalytic performance, *Separation and Purification Technology* 250 (2020) 117268.
- [25] J. Xie, M. Xu, R. Wang, S. Ye, X. Song, Three-Dimensional Porous Spherical $\text{TiO}_2\text{-Bi}_2\text{WO}_6$ Decorated Graphene Oxide Nanosheets Photocatalyst with Excellent Visible Light Catalytic Degradation of Ethylene, *Ceramics International* 47(10 Part A) (2021) 14183–14193.
- [26] A. Beeldens, An environmental friendly solution for air purification and self-cleaning effect: the application of TiO_2 as photocatalyst in concrete, *Proceedings of transport research arena Europe-TRA, Göteborg, Sweden* (2006).
- [27] H. Won Jang, A. Zareidoost, M. Moradi, A. Abuchenari, A. Bakhtiari, R. Pouriamanesh, B. Malekpouri, A. Jafari Rad, D. Rahban, Photosensitive nanocomposites: environmental and biological applications, *Journal of Composites and Compounds* 2(2) (2020) 50–61.
- [28] L. Bazli, M. Siavashi, A. Shiravi, A review of carbon nanotube/ TiO_2 composite prepared via sol-gel method, *Journal of Composites and Compounds* 1(1) (2019) 1–9.
- [29] I. Ali, M. Suhail, Z.A. Allothman, A. Alwarthan, Recent advances in syntheses, properties and applications of TiO_2 nanostructures, *Royal Society of Chemistry Advances* 8(53) (2018) 30125–30147.
- [30] M. Zhou, S. Roualdès, J. Zhao, V. Autès, A. Ayrat, Nanocrystalline TiO_2 thin film prepared by low-temperature plasma-enhanced chemical vapor deposition for photocatalytic applications, *Thin Solid Films* 589 (2015) 770–777.
- [31] L. Escobar-Alarcón, D.A. Solís-Casados, J. Perez-Alvarez, S. Romero, J.G. Morales-Mendez, E. Haro-Poniatowski, Preparation of Bi: TiO_2 thin films by an hybrid deposition configuration: pulsed laser deposition and thermal evaporation, *Applied Physics A* 117(1) (2014) 31–35.
- [32] H. Wang, X. Liu, X. Liu, Q. Guan, P. Huo, Y. Yan, Enhancement of photocatalytic activity on salicylic acid by nonmetal-doped TiO_2 with solvothermal method, *Desalination and Water Treatment* 54(9) (2015) 2504–2515.
- [33] D. Li, M. Wang, C. Luo, C. Pan, Preparation of TiO_2 -Coated Mo Powders for High Photocatalytic Property, *Journal of the American Ceramic Society* 99(1) (2015) 79–83.
- [34] R. Mohammadi, B. Massoumi, H. Eskandarloo, Preparation and characterization of Sn/Zn/TiO_2 photocatalyst for enhanced amoxicillin trihydrate degradation, *Desalination and Water Treatment* 53(7) (2015) 1995–2004.
- [35] D. Li, M. Wang, C. Luo, C. Pan, Preparation of TiO_2 -Coated Mo Powders for High Photocatalytic Property, *Journal of the American Ceramic Society* 99(1) (2016) 79–83.
- [36] M. Huang, S. Yu, B. Li, D. Lihui, F. Zhang, M. Fan, L. Wang, J. Yu, C. Deng, Influence of preparation methods on the structure and catalytic performance of SnO_2 -doped TiO_2 photocatalysts, *Ceramics International* 40(8, Part B) (2014) 13305–13312.
- [37] S.M. Gupta, M. Tripathi, A review on the synthesis of TiO_2 nanoparticles by solution route, *Central European Journal of Chemistry* 10(2) (2012) 279–294.
- [38] Y.M. Evtushenko, S.V. Romashkin, V.V. Davydov, Synthesis and properties of TiO_2 -based nanomaterials, *Theoretical Foundations of Chemical Engineering* 45(5) (2011) 731.
- [39] X. Chen, S.S. Mao, Titanium Dioxide Nanomaterials: Synthesis, Properties, Modifications, and Applications, *Chemical Reviews* 107(7) (2007) 2891–2959.
- [40] T.L. Thompson, J.T. Yates, Surface Science Studies of the Photoactivation of TiO_2 New Photochemical Processes, *Chemical Reviews* 106(10) (2006) 4428–4453.
- [41] M. Ferdosi Heragh, S. Eskandarinezhad, A. Dehghan, Ni-Cu matrix composite reinforced with CNTs: preparation, characterization, wear and corrosion behavior, inhibitory effects, *Journal of Composites and Compounds* 2(4) (2020) 123–128.
- [42] K. Elghniji, M. Ksibi, E. Elaloui, Sol-gel reverse micelle preparation and characterization of N-doped TiO_2 : Efficient photocatalytic degradation of methylene blue in water under visible light, *Journal of Industrial and Engineering Chemistry* 18(1) (2012) 178–182.

- [43] E.K.K.a.G.A.G. RAJ, Preparation, Characterization and Photocatalytic Behaviour of Codoped Nanophotocatalyst, *Chemical Science Transactions* 2(4) (2013) 1282-1287.
- [44] R.-C. Suci, M.C. Roşu, T.D. Silipaş, E. Indrea, V. Popescu, G.L. Popescu, Fe₃O₄-TiO₂ THIN FILMS PREPARED BY SOL-GEL METHOD, *Environmental Engineering & Management Journal (EEMJ)* 10(2) (2011) 187-192.
- [45] H. Choi, E. Stathatos, D.D. Dionysiou, Synthesis of nanocrystalline photocatalytic TiO₂ thin films and particles using sol-gel method modified with nonionic surfactants, *Thin Solid Films* 510(1–2) (2006) 107-114.
- [46] P. Kunwanlee, T. Puangpetch, S. Chavadej, Preparation and photocatalytic activity of mesoporous-assembled nano-titania thin films derived from a laurylamine hydrochloride surfactant-aided sol-gel method, *Materials Science in Semiconductor Processing* 26 (2014) 567-574.
- [47] G. Oskam, A. Nellore, R.L. Penn, P.C. Searson, The Growth Kinetics of TiO₂ Nanoparticles from Titanium(IV) Alkoxide at High Water/Titanium Ratio, *The Journal of Physical Chemistry B* 107(8) (2003) 1734-1738.
- [48] H.H. Kung, E.I. Ko, Preparation of oxide catalysts and catalyst supports — a review of recent advances, *The Chemical Engineering Journal and the Biochemical Engineering Journal* 64(2) (1996) 203-214.
- [49] C.J. Brinker, R. Sehgal, S.L. Hietala, R. Deshpande, D.M. Smith, D. Loy, C.S. Ashley, Sol-gel strategies for controlled porosity inorganic materials, *Journal of Membrane Science* 94(1) (1994) 85-102.
- [50] J.D. Mackenzie, E.P. Bescher, Chemical Routes in the Synthesis of Nanomaterials Using the Sol-Gel Process, *Accounts of Chemical Research* 40(9) (2007) 810-818.
- [51] Z. Goudarzi, N. Parvin, F. Sharifianjazi, Formation of hydroxyapatite on surface of SiO₂-P₂O₅-CaO-SrO-ZnO bioactive glass synthesized through sol-gel route, *Ceramics International* 45(15) (2019) 19323-19330.
- [52] M. Simonsen, E. Søgaard, Sol-gel reactions of titanium alkoxides and water: influence of pH and alkoxy group on cluster formation and properties of the resulting products, *Journal of Sol-Gel Science and Technology* 53(3) (2010) 485-497.
- [53] B. Yoldas, Hydrolysis of titanium alkoxide and effects of hydrolytic polycondensation parameters, *Journal of Materials Science* 21(3) (1986) 1087-1092.
- [54] J. Sekulic, J.E. ten Elshof, D.H.A. Blank, Synthesis and Characterization of Microporous Titania Membranes, *Journal of Sol-Gel Science and Technology* 31(1-3) (2004) 201-204.
- [55] N. Wetchakun, B. Incessungvorn, K. Wetchakun, S. Phanichphant, Influence of calcination temperature on anatase to rutile phase transformation in TiO₂ nanoparticles synthesized by the modified sol-gel method, *Materials Letters* 82(0) (2012) 195-198.
- [56] H. Choi, E. Stathatos, D.D. Dionysiou, Sol-gel preparation of mesoporous photocatalytic TiO₂ films and TiO₂/Al₂O₃ composite membranes for environmental applications, *Applied Catalysis B: Environmental* 63(1–2) (2006) 60-67.
- [57] E. Stathatos, P. Lianos, C. Tsakiroglou, Highly efficient nanocrystalline titania films made from organic/inorganic nanocomposite gels, *Microporous and Mesoporous Materials* 75(3) (2004) 255-260.
- [58] A. Attar, M. Ghamisari, F. Hajiesmaeilbaigi, S. Mirdamadi, Modifier ligands effects on the synthesized TiO₂ nanocrystals, *Journal of Materials Science* 43(5) (2008) 1723-1729.
- [59] C. Su, B.Y. Hong, C.M. Tseng, Sol-gel preparation and photocatalysis of titanium dioxide, *Catalysis Today* 96(3) (2004) 119-126.
- [60] V. Kessler, G. Spijksma, G. Seisenbaeva, S. Håkansson, D.A. Blank, H.M. Bouwmeester, New insight in the role of modifying ligands in the sol-gel processing of metal alkoxide precursors: A possibility to approach new classes of materials, *Journal of Sol-Gel Science and Technology* 40(2-3) (2006) 163-179.
- [61] E. Scolan, C. Sanchez, Synthesis and Characterization of Surface-Protected Nanocrystalline Titania Particles, *Chemistry of Materials* 10(10) (1998) 3217-3223.
- [62] R. Parra, M.S. Góes, M.S. Castro, E. Longo, P.R. Bueno, J.A. Varela, Reaction Pathway to the Synthesis of Anatase via the Chemical Modification of Titanium Isopropoxide with Acetic Acid, *Chemistry of Materials* 20(1) (2007) 143-150.
- [63] M. Ivanda, S. Musić, S. Popović, M. Gotić, XRD, Raman and FT-IR spectroscopic observations of nanosized TiO₂ synthesized by the sol-gel method based on an esterification reaction, *Journal of Molecular Structure* 480–481 (1999) 645-649.
- [64] C. Wang, Z.-X. Deng, Y. Li, The Synthesis of Nanocrystalline Anatase and Rutile Titania in Mixed Organic Media, *Inorganic Chemistry* 40(20) (2001) 5210-5214.
- [65] V. Salimian Rizi, F. Sharifianjazi, H. Jafarikhorami, N. Parvin, L. Saei Fard, M. Irani, A. Esmailkhanian, Sol-gel derived SnO₂/Ag₂O ceramic nanocomposite for H₂ gas sensing applications, *Materials Research Express* 6(11) (2019) 1150g2.
- [66] F.A. Harraz, O.E. Abdel-Salam, A.A. Mostafa, R.M. Mohamed, M. Hanafy, Rapid synthesis of titania-silica nanoparticles photocatalyst by a modified sol-gel method for cyanide degradation and heavy metals removal, *Journal of Alloys and Compounds* 551 (2013) 1-7.
- [67] M. Crişan, N. Drăgan, D. Crişan, A. Ianculescu, I. Niţoi, P. Oancea, L. Todan, C. Stan, N. Stănică, The effects of Fe, Co and Ni dopants on TiO₂ structure of sol-gel nanopowders used as photocatalysts for environmental protection: A comparative study, *Ceramics International* 42(2, Part B) (2016) 3088-3095.
- [68] R. Tang, Q. Jiang, Y. Liu, Preparation and Study on Photocatalytic Activity of N-doped TiO₂ Decorated N-doped graphene, *Procedia Engineering* 205 (2017) 573-580.
- [69] B. Palanisamy, C.M. Babu, B. Sundaravel, S. Anandan, V. Murugesan, Sol-gel synthesis of mesoporous mixed Fe₃O₄/TiO₂ photocatalyst: Application for degradation of 4-chlorophenol, *Journal of Hazardous Materials* 252–253 (2013) 233-242.
- [70] R. Roy, Accelerating the Kinetics of Low-Temperature Inorganic Syntheses, *Journal of Solid State Chemistry* 111(1) (1994) 11-17.
- [71] R.-C. Xie, J. Shang, Morphological control in solvothermal synthesis of titanium oxide, *Journal of Materials and Science* 42(16) (2007) 6583-6589.
- [72] A. Simpraditpan, T. Wirunmongkol, W. Boonwatharapunsakun, S. Pivsa-art, C. Duangduen, S. Sakulkhaemaruethai, S. Pavasupree, Preparation of High Photocatalyst Mesoporous TiO₂ from Nanosheets Using Autoclave Unit (Thai Made), *Energy Procedia* 9 (2011) 440-445.
- [73] A. Simpraditpan, T. Wirunmongkol, S. Pavasupree, W. Pecharapa, Effect of calcination temperature on structural and photocatalyst properties of nanofibers prepared from low-cost natural ilmenite mineral by simple hydrothermal method, *Materials Research Bulletin* 48(9) (2013) 3211-3217.
- [74] N. Liu, X. Chen, J. Zhang, J.W. Schwank, A review on TiO₂-based nanotubes synthesized via hydrothermal method: Formation mechanism, structure modification, and photocatalytic applications, *Catalysis Today* 225 (2014) 34-51.
- [75] X. Zhao, M. Liu, Y. Zhu, Fabrication of porous TiO₂ film via hydrothermal method and its photocatalytic performances, *Thin Solid Films* 515(18) (2007) 7127-7134.
- [76] G. Ren, Y. Gao, X. Liu, A. Xing, H. Liu, J. Yin, Synthesis of high-activity F-doped TiO₂ photocatalyst via a simple one-step hydrothermal process, *Reaction Kinetics, Mechanisms and Catalysis* 100(2) (2010) 487-497.
- [77] Y.B. Ryu, M.S. Lee, S.S. Park, G.-D. Lee, S.-S. Hong, Effect of synthesis temperature on the preparation of titanium dioxides by the hydrothermal method. Photocatalytic activity, *Reaction Kinetics and Catalysis Letters* 84(1) (2005) 101-108.
- [78] Y. Li, M. Zhang, M. Guo, X. Wang, Hydrothermal growth of well-aligned TiO₂ nanorod arrays: Dependence of morphology upon hydrothermal reaction conditions, *Rare Metals* 29(3) (2010) 286-291.
- [79] Y. Wang, L. Zhang, K. Deng, X. Chen, Z. Zou, Low Temperature Synthesis and Photocatalytic Activity of Rutile TiO₂ Nanorod Superstructures, *The Journal of Physical Chemistry C* 111(6) (2007) 2709-2714.
- [80] J. Ju, X. Chen, Y. Shi, J. Miao, D. Wu, Hydrothermal preparation and photocatalytic performance of N, S-doped nanometer TiO₂ under sunshine irradiation, *Powder Technology* 237 (2013) 616-622.
- [81] X. Shi, X. Yang, S. Wang, S. Wang, Q. Zhang, Y. Wang, Photocatalytic degradation of rhodamine B Dye with high purity anatase nano-TiO₂ synthesized by a hydrothermal method, *Journal of Wuhan University of Technology-Materials Science Edition* 26(4) (2011) 600-605.
- [82] J. Li, T. Wang, X. Du, Preparation of visible light-driven SnS₂/TiO₂ nanocomposite photocatalyst for the reduction of aqueous Cr(VI), *Separation and Purification Technology* 101 (2012) 11-17.
- [83] S.A.K. Leghari, S. Sajjad, F. Chen, J. Zhang, WO₃/TiO₂ composite with morphology change via hydrothermal template-free route as an efficient visible light photocatalyst, *Chemical Engineering Journal* 166(3) (2011) 906-915.
- [84] I. Tajzad, E. Ghasali, Production methods of CNT-reinforced Al matrix composites: a review, *Journal of Composites and Compounds* 2(2) (2020) 1-9.
- [85] S. Saadi, B. Nazari, Recent developments and applications of nanocomposites in solar cells: a review, *Journal of Composites and Compounds* 1(1) (2019) 41-50.
- [86] F.S. Jazi, N. Parvin, M. Tahriri, M. Alizadeh, S. Abedini, M. Alizadeh, The Relationship Between the Synthesis and Morphology of SnO₂-Ag₂O Nanocomposite, *Synthesis and Reactivity in Inorganic, Metal-Organic, and Nano-Metal Chemistry* 44(5) (2014) 759-764.
- [87] J. Liu, T. An, G. Li, N. Bao, G. Sheng, J. Fu, Preparation and characterization of highly active mesoporous TiO₂ photocatalysts by hydrothermal synthesis under weak acid conditions, *Microporous and Mesoporous Materials* 124(1–3) (2009) 197-203.
- [88] S. Ding, L. Wang, S. Zhang, Q. Zhou, Y. Ding, S. Liu, Y. Liu, Q. Kang, Hydrothermal synthesis, structure and photocatalytic property of nano-TiO₂-MnO₂, *Science in China Series B: Chemistry* 46(6) (2003) 542-548.
- [89] S.-H. Lee, M. Kang, S.M. Cho, G.Y. Han, B.-W. Kim, K.J. Yoon, C.-H.

- Chung, Synthesis of TiO₂ photocatalyst thin film by solvothermal method with a small amount of water and its photocatalytic performance, *Journal of Photochemistry and Photobiology A: Chemistry* 146(1–2) (2001) 121–128.
- [90] Y.-f. Wang, W.-y. Li, B. Zhou, X. Zhao, Synthesis and characterization of SnO₂-TiO₂ nanocomposite with rutile-phase via hydrothermal method at low temperature, *Chemical Research in Chinese Universities* 29(4) (2013) 617–620.
- [91] W. Kongsuechart, P. Praserttham, J. Panpranot, A. Sirisuk, P. Supphasri-rongjaroen, C. Satayaprasert, Effect of crystallite size on the surface defect of nano-TiO₂ prepared via solvothermal synthesis, *Journal of Crystal Growth* 297(1) (2006) 234–238.
- [92] C.T. Nam, W.-D. Yang, L.M. Duc, Study on photocatalysis of TiO₂ nanotubes prepared by methanol-thermal synthesis at low temperature, *Bulletin of Materials Science* 36(5) (2013) 779–788.
- [93] B. Liu, Y. Wang, Y. Huang, P. Dong, a.S. Yin, Morphological Control and Photocatalytic Activities of Nitrogen-doped Titania Nanoparticles by Microwave-assisted Solvothermal Process, *Journal of the Australian Ceramic Society* 48(2) (2012) 249–252.
- [94] K. Byrappa, T. Adschiri, Hydrothermal technology for nanotechnology, *Progress in Crystal Growth and Characterization of Materials* 53(2) (2007) 117–166.
- [95] R.E. Rimani, W.L. Suchanek, M.M. Lencka, Hydrothermal crystallization of ceramics, *Annales de Chimie Science des Matériaux* 27(6) (2002) 15–36.
- [96] S. Sömiya, R. Roy, Hydrothermal synthesis of fine oxide powders, *Bulletin of Materials Science* 23(6) (2000) 453–460.
- [97] A. Moghanian, F. Sharifianjazi, P. Abachi, E. Sadeghi, H. Jafarikhorami, A. Sedghi, Production and properties of Cu/TiO₂ nano-composites, *Journal of Alloys and Compounds* 698 (2017) 518–524.
- [98] T. Sugimoto, X. Zhou, A. Muramatsu, Synthesis of uniform anatase TiO₂ nanoparticles by gel–sol method: 3. Formation process and size control, *Journal of Colloid and Interface Science* 259(1) (2003) 43–52.
- [99] F. Wang, Z. Shi, F. Gong, J. Jiu, M. Adachi, Morphology Control of Anatase TiO₂ by Surfactant-assisted Hydrothermal Method, *Chinese Journal of Chemical Engineering* 15(5) (2007) 754–759.
- [100] M.S.N. Shahrababak, F. Sharifianjazi, D. Rahban, A. Salimi, A Comparative Investigation on Bioactivity and Antibacterial Properties of Sol-Gel Derived 58S Bioactive Glass Substituted by Ag and Zn, *Silicon* 11(6) (2019) 2741–2751.
- [101] X. Zhang, M. Zhou, L. Lei, Preparation of photocatalytic TiO₂ coatings of nanosized particles on activated carbon by AP-MOCVD, *Carbon* 43(8) (2005) 1700–1708.
- [102] M. Wojtoniszak, D. Dolat, A. Morawski, E. Mijowska, Carbon-modified TiO₂ for photocatalysis, *Nanoscale Research Letters* 7(1) (2012) 235.
- [103] W. Li, S. Ismat Shah, C.P. Huang, O. Jung, C. Ni, Metallorganic chemical vapor deposition and characterization of TiO₂ nanoparticles, *Materials Science and Engineering: B* 96(3) (2002) 247–253.
- [104] K.T. Raić, Formation of nanoparticles by CVD technique, *Metalurgija* 8(3) (2002) 191–200.
- [105] C.-S. Kuo, Y.-H. Tseng, C.-H. Huang, Y.-Y. Li, Carbon-containing nano-titania prepared by chemical vapor deposition and its visible-light-responsive photocatalytic activity, *Journal of Molecular Catalysis A: Chemical* 270(1–2) (2007) 93–100.
- [106] X. Zhang, M. Zhou, L. Lei, Preparation of an Ag–TiO₂ photocatalyst coated on activated carbon by MOCVD, *Materials Chemistry and Physics* 91(1) (2005) 73–79.
- [107] X. Zhang, M. Zhou, L. Lei, TiO₂ photocatalyst deposition by MOCVD on activated carbon, *Carbon* 44(2) (2006) 325–333.
- [108] G. Li Puma, A. Bono, D. Krishnaiah, J.G. Collin, Preparation of titanium dioxide photocatalyst loaded onto activated carbon support using chemical vapor deposition: A review paper, *Journal of Hazardous Materials* 157(2–3) (2008) 209–219.
- [109] J.H. Park, T.S. Sudarshan, Chemical vapor deposition, ASM international, Canada, 2001.
- [110] A.C. Jones, M.L. Hitchman, Chemical vapour deposition: precursors, processes and applications, Royal society of chemistry, England, 2009.
- [111] Y. Cao, X. Zhang, W. Yang, H. Du, Y. Bai, T. Li, J. Yao, A Bicomponent TiO₂/SnO₂ Particulate Film for Photocatalysis, *Chemistry of Materials* 12(11) (2000) 3445–3448.
- [112] C.W.H. Dunnill, Z.A. Aiken, J. Pratten, M. Wilson, D.J. Morgan, I.P. Parkin, Enhanced photocatalytic activity under visible light in N-doped TiO₂ thin films produced by APCVD preparations using t-butylamine as a nitrogen source and their potential for antibacterial films, *Journal of Photochemistry and Photobiology A: Chemistry* 207(2–3) (2009) 244–253.
- [113] R.Q. Cabrera, E.R. Latimer, A. Kafzas, C.S. Blackman, C.J. Carmalt, I.P. Parkin, Photocatalytic activity of needle-like TiO₂/WO_{3-x} thin films prepared by chemical vapour deposition, *Journal of Photochemistry and Photobiology A: Chemistry* 239(0) (2012) 60–64.
- [114] A. Sobczyk-Guzenda, B. Pietrzyk, H. Szymanowski, M. Gazicki-Lipman, W. Jakubowski, Photocatalytic activity of thin TiO₂ films deposited using sol–gel and plasma enhanced chemical vapor deposition methods, *Ceramics International* 39(3) (2013) 2787–2794.
- [115] S.-C. Jung, N. Imaishi, Preparation, crystal structure, and photocatalytic activity of TiO₂ films by chemical vapor deposition, *Korean Journal of Chemical Engineering* 18(6) (2001) 867–872.
- [116] H. Lee, M.Y. Song, J. Jung, Y.-K. Park, The synthesis and coating process of TiO₂ nanoparticles using CVD process, *Powder Technology* 214(1) (2011) 64–68.
- [117] W. Li, S. Ismat Shah, C.P. Huang, O. Jung, C. Ni, Metallorganic chemical vapor deposition and characterization of TiO₂ nanoparticles, *Materials Science and Engineering: B* 96(3) (2002) 247–253.
- [118] D.S. Bhachu, S. Sathasivam, C.J. Carmalt, I.P. Parkin, PbO-Modified TiO₂ Thin Films: A Route to Visible Light Photocatalysts, *Langmuir* 30(2) (2013) 624–630.
- [119] L. Lei, H.P. Chu, X. Hu, P.L. Yue, Preparation of Heterogeneous Photocatalyst (TiO₂/Alumina) by Metallo-Organic Chemical Vapor Deposition, *Industrial & Engineering Chemistry Research* 38(9) (1999) 3381–3385.
- [120] Z. Ding, X. Hu, G.Q. Lu, P.-L. Yue, P.F. Greenfield, Novel Silica Gel Supported TiO₂ Photocatalyst Synthesized by CVD Method, *Langmuir* 16(15) (2000) 6216–6222.
- [121] G.H. Kim, S.D. Kim, S.H. Park, Plasma enhanced chemical vapor deposition of TiO₂ films on silica gel powders at atmospheric pressure in a circulating fluidized bed reactor, *Chemical Engineering and Processing: Process Intensification* 48(6) (2009) 1135–1139.
- [122] P. Hajkova, P. Spatenka, J. Krumeich, P. Exnar, A. Kolouch, J. Matousek, The Influence of Surface Treatment on Photocatalytic Activity of PE CVD TiO₂ Thin Films, *Plasma Processes and Polymers* 6(S1) (2009) S735–S740.
- [123] S. Mathur, P. Kuhn, CVD of titanium oxide coatings: Comparative evaluation of thermal and plasma assisted processes, *Surface and Coatings Technology* 201(3–4) (2006) 807–814.
- [124] M.Y. Song, Y.-K. Park, J. Jung, Direct coating of V₂O₅/TiO₂ nanoparticles onto glass beads by chemical vapor deposition, *Powder Technology* 231(0) (2012) 135–140.
- [125] R.K. Bhakta, Rational development of precursors for MOCVD of TiO₂: precursor chemistry, thin film deposition, mechanistic studies, Dissertation, Bochum University, Germany, 2005.
- [126] A.C. Jones, Molecular design of improved precursors for the MOCVD of electroceramic oxides, *Journal of Materials Chemistry* 12(9) (2002) 2576–2590.
- [127] L.G. Hubert-Pfalzgraf, H. Guillon, Trends in precursor design for conventional and aerosol-assisted CVD of high-Tc superconductors, *Applied Organometallic Chemistry* 12(3) (1998) 221–236.
- [128] V.G. Bessergenev, R.J.F. Pereira, M.C. Mateus, I.V. Khmelinskii, D.A. Vasconcelos, R. Nicula, E. Burkel, A.M. Botelho do Rego, A.I. Saprykin, Study of physical and photocatalytic properties of titanium dioxide thin films prepared from complex precursors by chemical vapour deposition, *Thin Solid Films* 503(1–2) (2006) 29–39.
- [129] X.T. Yan, Y. Xu, *Chemical Vapour Deposition: An Integrated Engineering Design for Advanced Materials*, Springer London, China, 2010.
- [130] X.w. Zhang, M.h. Zhou, L.c. Lei, S. Xu, Synthesis of TiO₂ supported on activated carbon by MOCVD: operation parameters study, *Journal of Zhejiang University-SCIENCE A* 5(12) (2004) 1548–1553.
- [131] J.O. Choo, R. A. Adomaitis, G.W. Rubloff, L. Henn-Lecordier, Y. Liu, Simulation-based design and experimental evaluation of a spatially controllable CVD reactor, *American Institute of Chemical Engineers Journal* 51(2) (2005) 572–584.
- [132] K.L. Choy, Chemical vapour deposition of coatings, *Progress in Materials Science* 48(2) (2003) 57–170.
- [133] S. Bondi, W. Lackey, R. Johnson, X. Wang, Z. Wang, Laser assisted chemical vapor deposition synthesis of carbon nanotubes and their characterization, *Carbon* 44(8) (2006) 1393–1403.
- [134] P. O'Brien, N.L. Pickett, D.J. Otway, Developments in CVD Delivery Systems: A Chemist's Perspective on the Chemical and Physical Interactions Between Precursors, *Chemical Vapor Deposition* 8(6) (2002) 237–249.
- [135] M.W. Pyun, E.J. Kim, D.-H. Yoo, S.H. Hahn, Oblique angle deposition of TiO₂ thin films prepared by electron-beam evaporation, *Applied Surface Science* 257(4) (2010) 1149–1153.
- [136] N.T. Khoa, M.W. Pyun, D.H. Yoo, S.W. Kim, J.Y. Leem, E.J. Kim, S.H. Hahn, Photodecomposition effects of graphene oxide coated on TiO₂ thin film prepared by electron-beam evaporation method, *Thin Solid Films* 520(16) (2012) 5417–5420.

- [137] W.K. Lee, E.J. Kim, S.H. Hahn, Structural and photocatalytic properties of $\text{TiO}_2/\text{SiO}_x/\text{TiO}_x$ multi-layer prepared by electron-beam evaporation method, *Vacuum* 85(1) (2010) 30–33.
- [138] T.S. Yang, M.C. Yang, C.B. Shiu, W.K. Chang, M.S. Wong, Effect of N_2 ion flux on the photocatalysis of nitrogen-doped titanium oxide films by electron-beam evaporation, *Applied Surface Science* 252(10) (2006) 3729–3736.
- [139] S.W. Hsu, T.S. Yang, T.K. Chen, M.S. Wong, Ion-assisted electron-beam evaporation of carbon-doped titanium oxide films as visible-light photocatalyst, *Thin Solid Films* 515(7–8) (2007) 3521–3526.
- [140] P. Eiamchai, P. Chindaudom, A. Pokaipisit, P. Limsuwan, A spectroscopic ellipsometry study of TiO_2 thin films prepared by ion-assisted electron-beam evaporation, *Current Applied Physics* 9(3) (2009) 707–712.
- [141] T. Luttrell, S. Halpegamage, E. Sutter, M. Batzill, Photocatalytic activity of anatase and rutile TiO_2 epitaxial thin film grown by pulsed laser deposition, *Thin Solid Films* 564(0) (2014) 146–155.
- [142] P.B. Nair, V.B. Justinivictor, G.P. Daniel, K. Joy, V. Ramakrishnan, P.V. Thomas, Effect of RF power and sputtering pressure on the structural and optical properties of TiO_2 thin films prepared by RF magnetron sputtering, *Applied Surface Science* 257(24) (2011) 10869–10875.
- [143] C.H. Huang, C.C. Tsao, C.Y. Hsu, Study on the photocatalytic activities of TiO_2 films prepared by reactive RF sputtering, *Ceramics International* 37(7) (2011) 2781–2788.
- [144] C. Ma, W. Dong, L. Fang, F. Zheng, M. Shen, Z. Wang, Synthesis of $\text{TiO}_2/\text{Pt}/\text{TiO}_2$ multilayer films via radio frequency magnetron sputtering and their enhanced photocatalytic activity, *Thin Solid Films* 520(17) (2012) 5727–5732.
- [145] M.C. Wang, H.J. Lin, C.H. Wang, H.C. Wu, Effects of annealing temperature on the photocatalytic activity of N-doped TiO_2 thin films, *Ceramics International* 38(1) (2012) 195–200.
- [146] B. Barrocas, O.C. Monteiro, M.E.M. Jorge, S. Sérgio, Photocatalytic activity and reusability study of nanocrystalline TiO_2 films prepared by sputtering technique, *Applied Surface Science* 264(0) (2013) 111–116.
- [147] Z. Wang, N. Yao, X. Hu, X. Shi, Structural and photocatalytic study of titanium dioxide films deposited by DC sputtering, *Materials Science in Semiconductor Processing* 21(0) (2014) 91–97.
- [148] W. Zhang, K. Wang, S. Zhu, Y. Li, F. Wang, H. He, Yttrium-doped TiO_2 films prepared by means of DC reactive magnetron sputtering, *Chemical Engineering Journal* 155(1–2) (2009) 83–87.
- [149] C. Zhang, W. Ding, H. Wang, W. Chai, D. Ju, Influences of working pressure on properties for TiO_2 films deposited by DC pulse magnetron sputtering, *Journal of Environmental Sciences* 21(6) (2009) 741–744.
- [150] X. Yu, Z. Shen, Photocatalytic TiO_2 films deposited on cenosphere particles by pulse magnetron sputtering method, *Vacuum* 85(11) (2011) 1026–1031.
- [151] V. Meille, Review on methods to deposit catalysts on structured surfaces, *Applied Catalysis A: General* 315(0) (2006) 1–17.
- [152] A. Mubarak, E. Hamzah, M.R.M. Toff, Review of physical vapour deposition (PVD) techniques for hard coating, *Jurnal Mekanikal* 20(2) (2005) 42–51.
- [153] H.U. Krebs, M. Weisheit, J. Faupel, E. Súske, T. Scharf, C. Fuhse, M. Störmer, K. Sturm, M. Seibt, H. Kijewski, D. Nelke, E. Panchenko, M. Buback, Pulsed Laser Deposition (PLD)- A Versatile Thin Film Technique, in: B. Kramer (Ed.), *Advances in Solid State Physics*, Springer Berlin Heidelberg 2003, pp. 505–518.
- [154] A. Perrone, A. Zocco, L. Cultrera, D. Guido, Detailed studies of the plume deflection effect during long laser irradiation of solid targets, *Applied Surface Science* 197–198(0) (2002) 251–256.
- [155] Y. Suda, H. Kawasaki, T. Ueda, T. Ohshima, Preparation of high quality nitrogen doped TiO_2 thin film as a photocatalyst using a pulsed laser deposition method, *Thin Solid Films* 453–454(0) (2004) 162–166.
- [156] A. Khodorov, S. Levichev, A. Chahboun, A.G. Rolo, S. Bernstorff, N.P. Baradas, E. Alves, M.J.M. Gomes, Growth and characterization of Mn-doped ZnO/ TiO_2 multilayer nanostructures grown by pulsed laser deposition, *physica status solidi (c)* 7(11–12) (2010) 2724–2726.
- [157] S.-S. Lin, Y.-H. Hung, S.-C. Chen, The Properties of TiO_2 Nanoceramic Films Prepared by Electron Beam Evaporation, *Journal of Nanoscience and Nanotechnology* 9(6) (2009) 3599–3605.
- [158] Z. Lu, X. Jiang, B. Zhou, X. Wu, L. Lu, Study of effect annealing temperature on the structure, morphology and photocatalytic activity of Si doped TiO_2 thin films deposited by electron beam evaporation, *Applied Surface Science* 257(24) (2011) 10715–10720.
- [159] R. Schmidt, M. Parlak, A.W. Brinkman, Control of the thickness distribution of evaporated functional electroceramic NTC thermistor thin films, *Journal of Materials Processing Technology* 199(1–3) (2008) 412–416.
- [160] J. Singh, D.E. Wolfe, Review Nano and macro-structured component fabrication by electron beam-physical vapor deposition (EB-PVD), *Journal of Materials Science* 40(1) (2005) 1–26.
- [161] J.Z. Shi, C.Z. Chen, H.J. Yu, S.J. Zhang, Application of magnetron sputtering for producing bioactive ceramic coatings on implant materials, *Bulletin of Materials Science* 31(6) (2008) 877–884.
- [162] S.S. Lin, The optical properties of Ti-doped TiO_2 nanoceramic films deposited by simultaneous rf and dc magnetron sputtering, *Ceramics International* 38(4) (2012) 3129–3134.
- [163] Wenjie ZHANG, Shenglong ZHU, Y.L.a.F. WANG, Photocatalytic Property of TiO_2 Films Deposited by Pulse DC Magnetron Sputtering, *Journal of Materials Science and Technology –Shenyang* 20(1) (2004) 31–34.
- [164] V. Claudia, L. Francis, P.V. I, Photocatalytic degradation of acetone on ZnO-doped TiO_2 films prepared by sputtering, *Revue Roumaine de Chimie* 51(7–8) (2006) 827–833.
- [165] S.K. Zheng, T.M. Wang, G. Xiang, C. Wang, Photocatalytic activity of nano-structured TiO_2 thin films prepared by dc magnetron sputtering method, *Vacuum* 62(4) (2001) 361–366.
- [166] P. Pansila, N. Witit-anun, S. Chaikyakun, Influence of sputtering power on structure and photocatalyst properties of DC magnetron sputtered TiO_2 thin film, *Procedia Engineering* 32(0) (2012) 862–867.
- [167] Y. Song, J. Zhang, H. Yang, S. Xu, L. Jiang, Y. Dan, Preparation and visible light-induced photo-catalytic activity of H-PVA/ TiO_2 composite loaded on glass via sol–gel method, *Applied Surface Science* 292(0) (2014) 978–985.
- [168] M.Y. Abdelaal, R.M. Mohamed, Novel Pd/ TiO_2 nanocomposite prepared by modified sol–gel method for photocatalytic degradation of methylene blue dye under visible light irradiation, *Journal of Alloys and Compounds* 576(0) (2013) 201–207.
- [169] F. Oshani, R. Marandi, S. Rasouli, M.K. Farhoud, Photocatalytic investigations of TiO_2 -P25 nanocomposite thin films prepared by peroxotitanic acid modified sol–gel method, *Applied Surface Science* 311(0) (2014) 308–313.
- [170] Y. You, S. Zhang, L. Wan, D. Xu, Preparation of continuous TiO_2 fibers by sol–gel method and its photocatalytic degradation on formaldehyde, *Applied Surface Science* 258(8) (2012) 3469–3474.
- [171] T.S. Jamil, T.A. Gad-Allah, M.E.M. Ali, M.N.B. Momba, Utilization of nano size TiO_2 for degradation of phenol enrich water by solar photocatalytic oxidation, *Desalination and Water Treatment* 53(4) (2013) 1101–1106.
- [172] N. Abbas, G.N. Shao, M.S. Haider, S.M. Imran, S.S. Park, H.T. Kim, Sol–gel synthesis of TiO_2 - Fe_2O_3 systems: Effects of Fe_2O_3 content and their photocatalytic properties, *Journal of Industrial and Engineering Chemistry* 39 (2016) 112–120.
- [173] I. Singh, R. Kumar, B.I. Birajdar, Zirconium doped TiO_2 nano-powder via halide free non-aqueous solvent controlled sol-gel route, *Journal of Environmental Chemical Engineering* 5(3) (2017) 2955–2963.
- [174] S.I. Al-Mayman, M.S. Al-Johani, M.M. Mohamed, Y.S. Al-Zeghayer, S.M. Ramay, A.S. Al-Awadi, M.A. Soliman, TiO_2 ZnO photocatalysts synthesized by sol–gel auto-ignition technique for hydrogen production, *International Journal of Hydrogen Energy* 42(8) (2017) 5016–5025.
- [175] A.C. Martins, A.L. Cazzetta, O. Pezoti, J.R.B. Souza, T. Zhang, E.J. Pilau, T. Asefa, V.C. Almeida, Sol-gel synthesis of new TiO_2 /activated carbon photocatalyst and its application for degradation of tetracycline, *Ceramics International* 43(5) (2017) 4411–4418.
- [176] W.H. Yuan, Z.L. Xia, L. Li, Synthesis and photocatalytic properties of core-shell TiO_2 @ ZnIn_2S_4 photocatalyst, *Chinese Chemical Letters* 24(11) (2013) 984–986.
- [177] N.R. Khalid, E. Ahmed, Z. Hong, M. Ahmad, Synthesis and photocatalytic properties of visible light responsive La/ TiO_2 -graphene composites, *Applied Surface Science* 263(0) (2012) 254–259.
- [178] Z. He, W. Que, J. Chen, X. Yin, Y. He, J. Ren, Photocatalytic Degradation of Methyl Orange over Nitrogen–Fluorine Codoped TiO_2 Nanobelts Prepared by Solvothermal Synthesis, *ACS Applied Materials & Interfaces* 4(12) (2012) 6816–6826.
- [179] H.R. Pant, B. Pant, R.K. Sharma, A. Amarjargal, H.J. Kim, C.H. Park, L.D. Tijing, C.S. Kim, Antibacterial and photocatalytic properties of Ag/ TiO_2 /ZnO nano-flowers prepared by facile one-pot hydrothermal process, *Ceramics International* 39(2) (2013) 1503–1510.
- [180] M. Yao, J. Zhao, S. Lv, K. Lu, Preparation and hydrogenation of urchin-like titania using a one-step hydrothermal method, *Ceramics International* 43(9) (2017) 6925–6931.
- [181] S. Min, J. Hou, Y. Lei, X. Ma, G. Lu, Facile one-step hydrothermal synthesis toward strongly coupled TiO_2 /graphene quantum dots photocatalysts for efficient hydrogen evolution, *Applied Surface Science* 396 (2017) 1375–1382.
- [182] R. Hao, G. Wang, C. Jiang, H. Tang, Q. Xu, In situ hydrothermal synthesis of g- C_3N_4 / TiO_2 heterojunction photocatalysts with high specific surface area for Rhodamine B degradation, *Applied Surface Science* 411 (2017) 400–410.

- [183] U. Alam, M. Fleisch, I. Kretschmer, D. Bahnemann, M. Muneer, One-step hydrothermal synthesis of Bi-TiO₂ nanotube/graphene composites: An efficient photocatalyst for spectacular degradation of organic pollutants under visible light irradiation, *Applied Catalysis B: Environmental* 218(0) (2017) 758-769.
- [184] Z. Tian, N. Yu, Y. Cheng, Z. Wang, Z. Chen, L. Zhang, Hydrothermal synthesis of graphene/TiO₂/CdS nanocomposites as efficient visible-light-driven photocatalysts, *Materials Letters* 194 (2017) 172-175.
- [185] C.C. Chen, W.J. Yang, C.Y. Hsu, Investigation into the effects of deposition parameters on TiO₂ photocatalyst thin films by rf magnetron sputtering, *Superlattices and Microstructures* 46(3) (2009) 461-468.
- [186] S.-J. Shen, T.-S. Yang, M.-S. Wong, Co-sputtered boron-doped titanium dioxide films as photocatalysts, *Surface and Coatings Technology* 303 (2016) 184-190.
- [187] M. Lelis, S. Tuckute, S. Varnagiris, M. Urbonavicius, G. Laukaitis, K. Bockute, Tailoring of TiO₂ film microstructure by pulsed-DC and RF magnetron co-sputtering, *Surface and Coatings Technology* 377 (2019) 124906.